UNIVERSITÀ DEGLI STUDI DI MILANO

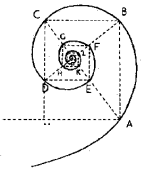

SCUOLA DI DOTTORATO IN MEDICINA MOLECOLARE

CICLO XXVI

Anno Accademico 2012/2013

TESI DI DOTTORATO DI RICERCA

BIO/10

Sphingolipid signaling as a target in photoreceptor degeneration: an *in vitro* model for therapeutic strategies in Retinitis Pigmentosa

Dottorando: Dr.ssa Carlotta Fabiani

Matricola R09147

TUTORE: Prof. Riccardo Ghidoni

DIRETTORE DEL DOTTORATO: Prof. Mario Clerici

Ai miei genitori,

per essere, da sempre, il mio porto sicuro.

A Chico

per tutto l'amore con cui, quotidianamente,
riempie il nostro mondo.

Si diventa molto più fortil
là dove ci si spezza…

ABSTRACT

Background: *Sphingolipids are a broad class of molecules with the double role of cell membranes components and intra/extra cellular signal mediators, controlling proliferation, differentiation, stress survival and apoptosis. Ceramide (Cer), the core of complex sphingolipids, can undergo deacylation giving rise to sphingosine and sphingosine-1-phosphate (S1P). This latter exerts a pro-survival and proliferative activity, as opposed to Cer, which promotes cell cycle arrest and apoptosis. Retinal degeneration and in particular Retinitis Pigmentosa (RP) are associated to Cer accumulation and cell death induction. In a murine model of RP (rd10 mutant mice), it has been demonstrated that inhibition of Cer synthesis and accumulation, blocking serine palmitoyltransferase (SPT) with Myriocin, rescues retinal photoreceptors, especially cones, from degeneration.*

Aim: *Our aim is to target sphingolipid metabolism to reduce retinal photoreceptor damage, in a cone photoreceptors cell line. In particular, promoting S1P intracellular increase by S1Plyase inhibition and Cer depletion through SPT inactivation.*

Methods: *Murine 661W cone-like cell line were treated with 75μM 2-acetyl-4(5)-(1(R),2(S),3(R),4-tetrahydroxybutyl)-imidazole (THI), an inhibitor of S1Plyase, for 2 hours; next, cells were starved and treated with 1mM H_2O_2 for different times. Cell growth curve was determined by MTT assay and viability with Trypan blue. TUNEL assay and FRAP test were employed to verify, respectively, apoptosis degree and antioxidant-intrinsic power. Sphingolipid intracellular amounts were measured through LC-MS analysis. ERK1/2 and Akt/PKB phosphorylation, Bcl-2/Bax ratio and Nrf2 expression was evaluated by Western blotting with specific antibodies. Real time-PCR was performed to establish HO-1 and S1P receptors transcript changes upon THI and oxidative stress treatments. Exogenous S1P (100nM) and Myriocin (10μM) were also employed, respectively 1 hour and 5 hours before H_2O_2, to antagonize oxidative stress effect on photoreceptors. Lastly, we screened 30 new synthetic compounds to determine their ability in inhibiting SPT, through an enzymatic activity assay.*

Results: *We show that enhanced stability of S1P, obtained through THI administration, reduces inhibitory starvation and H_2O_2 effect on cell proliferation and viability. In particular, through THI ability to reverse stresses-induced ERK1/2 dephosphorylation and Akt phosphorylation on Ser473. We focused our investigations on oxidative stress, finding that THI counteracts H_2O_2-induced apoptosis increasing Bcl-2/Bax ratio and antioxidant-intrinsic power modulating Nrf2/HO-1 pathway. Furthermore, THI differentially induces S1P receptors transcript expression, showing the major effect on S1P4 and S1P5. In addition, low exogenous S1P improves 661W proliferation, viability and antioxidant response, whereas higher concentration leads to S1P receptors saturation. Myriocin treatment, either alone or in combination with THI, rescues photoreceptors from H_2O_2-induced oxidative stress and drastically reduces all Cer pools. Simultaneously, we selected three compounds with inhibitory activity on SPT, showing an IC50 values ranging from 17.71μM to 40.41μM.*

Conclusions: *We conclude that S1P stabilization and, in general, sphingolipid metabolism manipulation can be considered a therapeutic target in order to*

promote photoreceptors survival under different stress conditions, such as oxidative stress.

RIASSUNTO

Introduzione: *gli Sfingolipidi sono una vasta famiglia di molecole con il duplice ruolo di componenti strutturali di membrane e mediatori intra ed extra cellulari. Sono implicati nel controllo di proliferazione, differenziazione e sopravvivenza cellulare ma anche di fenomeni legati alla morte, tra cui l'apoptosi. Ceramide (Cer), alla base degli sfingolipidi complessi, può andare incontro a deacilazione generando sfingosina e sfingosina-1-fosfato (S1P). Quest'ultimo è considerato un mediatore di sopravvivenza e proliferazione cellulare, in opposizione a Cer, che promuove arresto del ciclo ed apoptosi. La degenerazione retinica ed, in particolare la Retinite Pigmentosa (RP) sono associate all'accumulo di Cer ed all'induzione di morte cellulare. L'inibizione della sintesi e dell'accumulo di Cer, inattivando la serina palmitoiltransferasi (SPT) attraverso l'utilizzo di Miriocina, è stata dimostrata essere coinvolta nel recupero morfologico e funzionale dei fotorecettori retinici, in particolare dei coni, in un modello murino di RP (mutante rd10).*

Scopo: *Il nostro scopo è di intervenire sul metabolismo degli sfingolipidi per ridurre il danno di fotorecettori retinici, attarveso l'utilizzo di una linea cellulare di fotorecettori coni. In particolare, promuovendo l'aumento di S1P intracellulare, tramite l'inibizione dell'enzima S1P liasi, e la riduzione di Cer attraverso l'inattivazione di SPT.*

Metodi: *le cellule murine 661W, una linea di fotorecettori (coni), sono state trattate con 2-acetil-4(5)-(1(R),2(S),3(R),4-tetraidrobutil)-imidazolo (THI) 75μM, un inibitore dell'enzima S1Pliasi, per 2 ore; quindi, le cellule sono state sottoposte a deprivazione di siero e trattate con H_2O_2 1mM per differenti lassi di tempo. La curva di crescita di queste cellule è stata determinata attraverso il saggio MTT e la vitalità con Typan blue. Il saggio TUNEL e il FRAP test sono stati impiegati per verificare, rispettivamente, il grado di apoptosi e il potere antiossidante intrinseco dei fotorecettori. I contenuti intracellulari di sfingolipidi sono stati misurati attraverso l'analisi LC-MS. La tecnica del Western blotting, attraverso l'impiego di anticorpi specifici, è stata utilizzata per valutare la fosforilazione di ERK1/2 e Akt/PKB, il rapporto tra Bcl-2/Bax e l'espressione proteica di Nrf2. Attraverso Real time-PCR, le modulazioni nell'espressione dei trascritti di HO-1 e dei recettori di S1P sono stati valutati in seguito a stress ossidativo e trattamento con THI. S1P esogeno (100nM) e Miriocina (10μM) sono stati impiegati, rispettivamente 1 ora e 5 ore prima H_2O_2, per antagonizzare l'effetto dello stimolo ossidativo sui fotorecettori. In fine, abbiamo esaminato 30 composti di nuova sintesi per determinare la loro capacità inibitoria su SPT, attraverso un saggio di attività enzimatica.*

Risultati: *i nostri risultati mostrano che l'aumentata stabilità di S1P, ottenuta tramite l'utilizzo di THI, è in grado di ridurre l'effetto inibitorio sulla proliferazione e la vitalità cellulare, dato dalla deprivazione di siero e dal trattamento con H_2O_2. Il pretrattamento con THI, infatti, antagonizza la de-fosforilazione di ERK1/2 e la fosforilazione di Akt su Ser473, indotte dagli stimoli di morte utilizzati. Abbiamo, quindi, focalizzato la nostra ricerca sugli effetti dello stress ossidativo, evidenziando che THI si contrappone all'induzione dell'apopstosi tramite l'aumento del rapporto Bcl-2/Bax e influenza il potere antiossidante intrinseco dei fotorecettori modulando la via di segnale di Nrf2 e HO-1. Inoltre, THI aumenta l'espressione dei recettori di S1P, mostrando un effetto maggiore sui recettori S1P4 e S1P5. Inoltre,*

abbiamo osservato che basse concentrazioni di S1P migliorano la proliferazione, la vitalità e la risposta antiossidante di cellule 661W, mentre alte concentrazioni portano alla saturazione dei recettori.Il pretrattamento con miriocina, sia da solo che in combinazione con THI, protegge i fororecettori dallo stress ossidativo e riduce drasticamente i livelli intracellulari di tutte le specie di Cer. Parallelamente, abbiamo selezionato tre composti con attività inbitoria su SPT, determinando i rispettivi valori di IC50 che sono risultati essere compresi tra 17,71μM e 40,41μM.
Conclusioni: *possiamo quindi concludere che la stabilizzazione di S1P e, più in generale, l'azione sul metabolismo degli sfingolipidi è da considerarsi un target terapeutico per promuovere la sopravvivenza fotorecettoriale in differenti condizioni di stress, tra cui lo stress ossidativo.*

INDEX

SIMBOL LIST

3-KdhSph	3-ketodihydrosphingosine
3-KSR	3-ketosphinganine reductase
ABCC1	ATP binding cassette C1
AC (aCDase)	Acid Ceramidase
adRP	Autosomal dominant RP
Akt/PKB	Akt/Protein kinase B
AMD	Age-related macular degeneration
arRP	Autosomal recessive RP
ASMase (aSMase)	Acid sphingomyelinase
Bax	BCL (B Cell Lymphoma)-Associated X
BDNF	Brain derived neurotrophic factor
BH3	Bcl-2 homology 3
C1P	Ceramide-1-phosphate
CA	Carnosic acid
CAPE	Caffeic acid phenethyl ester
Cer	Ceramide
Cer.s	Ceramides
CERK	Ceramide kinase
CERKL	Ceramide kinase-like protein
CerS	Ceramide synthase
CerSs	Ceramide synthases
CERT	Ceramide transport protein
CFTR	Cystic fibrosis transmembrane regulator
cGMP	Cyclic guanosine monophosphate
ChR2	Channelrhodopsin-2
CNTF	Ciliary neurotrophic factor
CPE	Ceramide phosphoethanolamine
CRalBP	Cellular retinaldehyde binding protein
DES	Dihydroceramide desaturase
DHA	Docosahexaenoic acid
dhCer	Dihydroceramide
dhCerS	Dihydroceramide synthase
dhCers	Dihydroceramides
dhCerSs	Dihydroceramide synthases
dhSph	Dihydrosphingosine
EDG	Endothelial differentiation gene
ER	Endoplasmatic reticulum
ERG	Electroretinography
ERK	Extracellular signal-regulated kinases
ES	Electrical stimulation
GalCer	Galactosyl Ceramide
GAPDH	Glyceraldehyde-3-phosphate dehydrogenase
GCase	Glucocerebrosidase

GCS	Glucosylceramide synthase
GDNF	Glial cell derived neurotrophic factor
GluCer	Glucosylceramide
GPCR	G protein-coupled receptor
GSLs	Glycosphingolipids
GTP	Guanosine-5'-triphosphate
H_2O_2	Hydrogen peroxide
Hex	Hexadecenal
HO-1	Heme oxygenase-1
IOP	Intraocular pressure
IRBP	Inter-photoreceptor retinal binding protein promoter
JNK	c-Jun N-terminal kinases
MAPK	Mitogen-activated protein kinase
MDA	Malondialdehyde
NAPDH	Nicotinamide adenine di nucleotide phosphate
NC (nCDase)	Neutral Ceramidase
NF-Kb	Nuclear factor Kb
NGF	Nerve grwth factor
Nrf2	NF-E2-related factor 2
NSMase (nSMase)	Neutral sphingomyelinase
PC	Phosphatidylcholine
PDE	Phosphodiesterase
PE (EA1P)	Phosphoethanolamine
PEDF	Pigment epithelium derived factor
PKC	Protein kinase C
PLP	Pyridoxal 5'-phosphate
PM	Plasma membrane
PP1	Protein phosphatases 1
PP2A	Protein phosphatases 2A
PRE	Purple rice bran extract
PUFA	Polyunsatured fatty acid
RGCs	Retinal ganglion cells
RHO	Rhodopsin
RONS	Reactive oxygen and nitrogen species
ROS	Reactive oxygen species
RP	Retinitis Pigmentosa
RPE	Retinal pigment epithelium
RPE65	Retinal pigment epithelium specific protein 65kDa
S1P	Sphingosine-1-phospate
S1P1	Sphingosine-1-phosphate receptor 1
S1P2	Sphingosine-1-phosphate receptor 2
S1P3	Sphingosine-1-phosphate receptor 3
S1P4	Sphingosine-1-phosphate receptor 4
S1P5	Sphingosine-1-phosphate receptor 5

S1PRs	Sphingosine-1-phosphate receptors
SD	Serum deprivation
SM	Sphingomyelin
SMS1/2	Sphingomyelin synthase 1/2
SMSr	Sphingomyelin synthase-related protein
Sph	Sphingosine
Sphk1-2 (SK1/2)	Sphingosine kinase 1 -2
SPL	Sphingosine-1-phosphate lyase
SPLs	Sphingolipids
SPP	Sphingosine-1-phosphate phosphatase
SPT	Serine palmitoyltransferase
sSMase	Secretory sphingomyelinase
TES	Transcorneal electrical stimulation
THI	2-acetyl-4(5)-(1(R),2(S),3(R),4-tetrahydroxybutyl)-imidazole
TNFα	Tumour necrosis factor α
UPR	Unfolded protein response
XLRP	X-linked RP

FIGURE LIST

1. INTRODUCTION

1.1 Retina

The retina, or eye nervous tunic, is placed in the posterior segment of the eye, between the vitreous body and the vascular tunic. It is a multilayer structure mostly comprised of neural cells and crossed by Müller cells, representing the retinal glia.

It is the neural portion of the eye and belongs to the central nervous system, although its peripheral anatomic position. It structurally arises from the diencephalon, which is connected through the optic nerve, that refolds originating the *optic vesicle*, and consequently the *optic cup*: whose inner wall corresponds to the retina whereas the outer becomes the pigment epithelium (RPE). The epithelium is made up of a tight-junction, connected, single cell layer in close contact with the external retinal neurons, photoreceptors, and separated from the choroid by the Bruch's membrane, the blood-retina barrier. RPE apical membrane and processes surround the light-sensitive outer segments of photoreceptors establishing a tight structural and functional relationship. Because of high melanin content, it represents a sort of shield for entering light; furthermore, its thigh relation with photoreceptors involves it in several metabolic activities with critical relevance in photoreceptors survival, such as: release of neurotrophic factors and nutrients and daily phagocytosis of outer segments to prevent retinoids derivates and oxidized lipid accumulation, in RPE cells also visual cycle occurs [1].

Five are the typologies of neurons present in the retina. Starting from the pigment epithelium we find: photoreceptors, the light-sensitive cells; bipolar cells and ganglion cells (RGCs), whose axons bundle to form the optic nerve. The nervous signal arises in photoreceptors after light stimulus and goes through this three-neurons chain, crossing the optic nerve, directly to the visual cortex in the central nervous system. The other two kinds of neural cells are the horizontal and the amacrine; they are, respectively,

responsible for lateral interactions of photoreceptor-bipolar cells and bipolar-ganglion cells synapses, originating the so called ribbon synapses. The neural retina can be divided into six layers distinguished by the kind or the structure of cells that it houses: photoreceptors outer segments layer; outer nuclear layer, with photoreceptors nuclei; outer plexiform layer, where photoreceptors make synapse with bipolar and horizontal cells; inner nuclear layer, containing bipolar, horizontal and amacrine nuclei; inner plexiform layer, where there are the synapses of photoreceptors or amacrine cells with ganglion cells and finally ganglion cell layer, occupying from their nuclei (Fig. 1.1) [2].

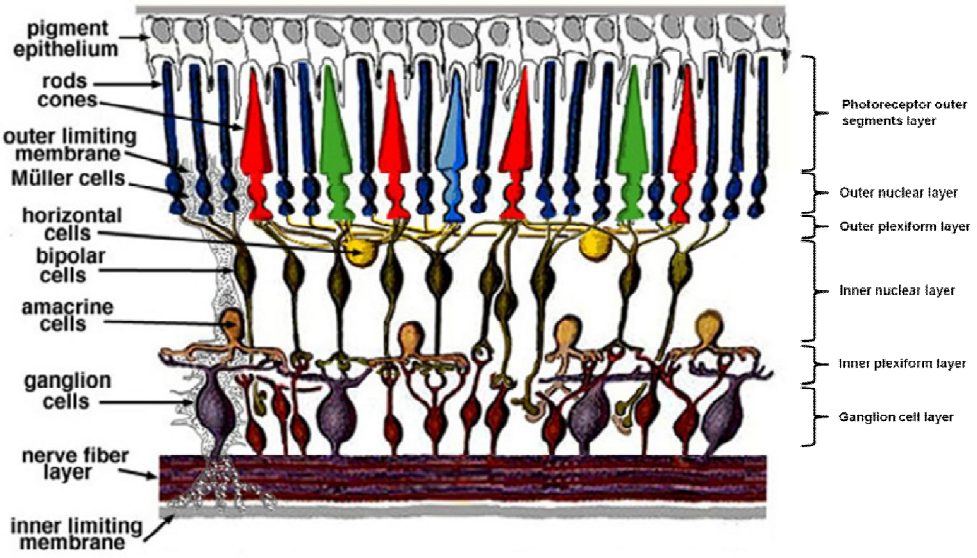

Fig. 1.1: Schematic representation of neural retinal cell layers. Modified from: *www.webvsion.med.utah.edu*

1.1.1 Photoreceptors

The photoreceptors are the retinal neurons, where the phototransduction cascade is activated. Their cellular structure could be described dividing it into two major parts: an outer segment, specialized in detecting photons signal and constituted of stacks of disk membranes in which cromophores

are localized, and an inner segment, containing the nucleus and other cellular organelles necessary for cell metabolism.

Photoreceptors can be distinguished in two classes: rods and cones. Their complementarity is described in several traits in which they differ: number, retinal distribution, structure, function and sensitivity to light .

Due to their sensitivity to light, rods, with their slim and protracted structure, are able to detect a single incoming photon and therefore their function consists in allowing vision under dark-dim conditions at night (scotopic vision). On the other hand, cones, robust conical-shaped and shorter than rods, are up to 100-fold less sensitive than rods but show an extraordinary ability in adjusting their sensitivity and are fundamental for colour perception in our visual image (photopic vision). Their specific and opposite roles, bring to rods saturation in bright light and to inactivation of cones in darkness. [3]. They differ also in number and retinal distribution, cones are mainly concentrated, organized in a hexagonal mosaic, in the central area, the fovea, and do not exceed 6-7 million of cells. On the other hand rods are distributed all across the retina and, even if they maintain a regular architecture, they do not follow a real defined distribution. Rods are much more numerous, they can reach a total of up to 120 million of cells [4].

1.1.2 Phototransduction

Phototransduction is the signal transduction pathway whereby incoming light is transformed in electrical response. The key proteins starting this mechanism are retinal chromophores, rhodopsin in rods and three different wavelength sensitive-opsins in cones, long wavelength sensitive for red (L-cones), middle wavelength sensitive for green (M-cones) and short wavelength sensitive for blue (S-cones). Absorption of a photon by retinal cromophores cause the isomerization of 11-*cis* retinal to all-*trans* retinal and the start of the phototransduction cascade. This conformational change

brings to the dissociation of the prostatic group from the opsin, that binds and stimulates a GTP binding protein, transducin, inducing the activation of its α-subunit. The activated transducin subunit binds to the enzyme cGMP phosphodiesterase (PDE) that gradually hydrolyzes cytoplasmatic cGMP and leads to the closure of cGMP-gated channels on the plasma membrane (PM) (Fig. 1.2). These channels maintain a steady inward current in darkness ("dark current") and depolarize the cell sufficiently (dark membrane potential at ~−30 mV) to sustain synaptic-transmitter (glutamate) release. The light-induced closure of the cGMP-gated channels produces a reduction of positive ions concentration (Na^+ and Ca^{++}) inside the outer segment and a consequent membrane hyperpolarization. The generated electric current crosses the photoreceptor body up to the synaptic terminal, reducing or stopping glutamate release and secondary neurons inhibition [5].

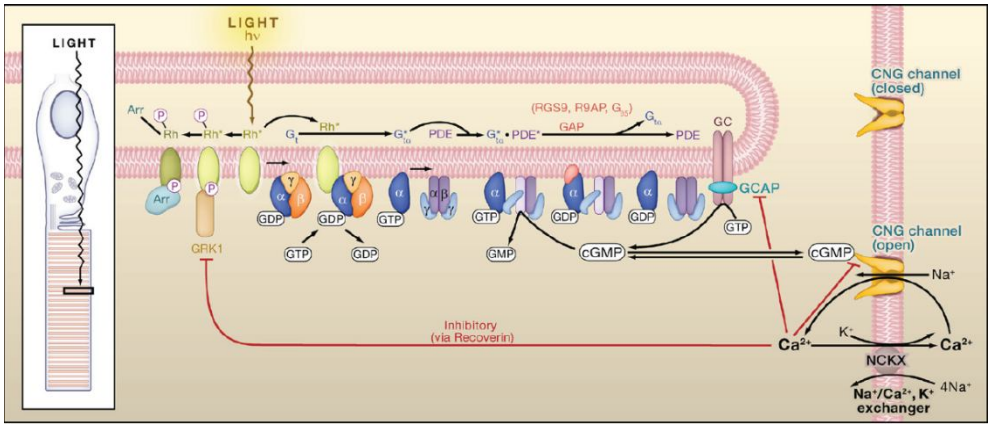

Fig. 1.2: Schematic representation of phototransduction cascade. Original source: *Yau et al 2009*

Along with phototransduction, visual cycle occurs in RPE photoreceptors-adjacent cells. This fundamental process implicated in cromophores recycling, covers an important role, not only in guaranteeing a prompt

transformation of all-*trans* retinal back in 11-*cis* retinal, necessary for an efficient response to light, but also in protecting photoreceptors against bis-retinoids and adducts possible accumulation [6].

1.1.3 Retinal degenerations: Retinitis Pigmentosa

Due to its complexity, the retina is exposed to several kind of degenerations, generally distinguishable by the first kind of cell layer affected but often extended to others retinal structures. This underlies how critically important is the equilibrium between all cells that constitute the retina. Some of the most studied pathologies are linked below.

Age-related macular degeneration (AMD), in which photoreceptors placed in the macula, the central area of the retina, start to degenerate in later-life, seems to be related both with neovascularization and RPE dysfunctions that leads to the accumulation of extracellular deposits between epithelial cells and Brunch's membrane. This induces the block of nutrients and regulatory substances fluxes, which are vital for RPE and photoreceptor survival. Glaucoma, characterized by an elevation of intraocular pressure (IOP), shows a degeneration of RGCs and optic nerve head, rapidly translated in loss of visual fields. Diabetic retinopathy is tightly connected with neovascularization, caused by hyperglycaemia-induced microvascular occlusion. As well as in AMD, new vessels invade RPE and branch out inside the neuroretina [7]. Retinitis Pigmentosa (RP) is one of the most common forms of inherited pathologies that affects retinal tissues and, probably, the most complex and heterogeneous studied. RP includes a group of inherited retinal disorders, in which loss of photoreceptors and retinal pigment deposits are observed. It, characteristically, starts with rod loss, linked to poor night vision, and then evolves in progressive cone degeneration causing the reduction of mid-peripheral field of vision. Still-active area, gradually, shrinks into a small central region corresponding to

macular cones and defining the typical tunnel vision described in these kinds of pathologies. Final-point patients lose the central vision in later-life and can reach legal and, at last, total blindness. RP could be classified in three wide groups: simple, when only eye dysfunctions are identified; syndromic, in the case of, also, non-ocular disease are implicated and systemic, related to pathologies in which retinal degeneration becomes less relevant than other organs involvement. Some of the most studied syndromes linked to RP are Usher's syndrome, Bardet-Biedl syndrome, Leber's congenital amaurosis and Refsum's disease [8] [9].

1.1.3.1 Genetic mutations

Three are the main kinds of inherited transmission in RP, almost of monogenic mutations (deletions, insertions or substitutions): autosomal-dominant (20-25%), autosomal-recessive (15-20%) and X-linked (10-15%). The residual percentage is represented by non-genetic factors, non-Mendelian inheritance (for example mitochondrial or *de novo* mutations) and complex inheritance. Some patients present digenic RP (one modification in RDS gene, encoding peripherin, and another in ROM1 gene, encoding retinal outer segment membrane protein 1) [10].
Since 1984, when the first polymorphism was associated to RP [11], more than 50 genes, linked to non-syndromic RP, were mapped and identified (Tab. 1.1).

RP Category	Total Genes and Loci	Identified Genes
Autosomal dominant (adRP)	20	19
Autosomal recessive (arRP)	32	29
X-linked (XLRP)	5	2

Tab. 1.1: Number of genes associated to non-syndromic retinitis pigmentosa. Original source: *https://sph.uth.edu/retnet/sum-dis.htm#D-graph*

Genetic mutations resulting in photoreceptors degeneration can affect genes implicated in several functions: renewal and shedding of outer segment, as mutation in peripherin/RDS gene, one of the earliest protein linked to RP [12, 13]; visual transduction cascade, as mutated phosphodiesterase catalytic subunits α (PDE6A) and β (PDE6B) and five different mutations of rod cGMP-gated channel, both kind of mutations related to arRP; metabolism of retinol, as mutation in cellular retinaldehyde-binding protein (CRalBP) or in retinal pigment epithelium protein (RPE65) [14]. One of the most studied retinal protein is the rhodopsin (RHO), the first found to be mutated in RP [15] and the responsible for almost 25% of adRP cases. Many different mutations, divided in six classes, are related to this protein giving rise to patients extensive clinical heterogeneity [16]. Among all numerous mutations causing arRP one is particularly relevant for our study. In RP26, an autosomal recessive locus, it was identified a mutation linked to CERKL gene, encoding a modified ceramide kinase-like protein able to augment the sensibility of retinal cells to apoptotic stimuli. This outcome determines the first link between human genetic modification of sphingolipid metabolism and the onset of retinal degeneration [17].

1.1.3.2 Mechanisms of photoreceptors degeneration

Photoreceptors vulnerability is particularly enhanced by their peculiar physiology and biochemistry, keeping them on a fine line between survival and death, where any defect can be crucial in defining their fate. The first factor that subjects photoreceptors to risks is light exposure. In presence of oxygen, the ionizing effect of light is boosted and reactive oxygen and nitrogen species (RONS) are generated especially by photosensitizing molecules, such as retinoids. Both retinoid derivates and RONS excessive accumulation can cause photoreceptor degeneration. Another source of vulnerability in photoreceptors is represented by their lipid-rich outer segment membranes, especially for very-long-chain polyunsaturated fatty acid (PUFA). PUFAs oxidation gives rise to highly reactive electrophilic aldehydes, including malondialdehyde (MDA) that starts destructive free radical chain reactions. Moreover, retinal protein mutations, especially linked to RHO, cause protein misfolding activating the unfolded protein response (UPR) in the endoplasmatic reticulum (ER). All this events can similarly subject photoreceptors to oxidative stress which represents one of the most studied death stimulus to be counteracted in retinal degenerations [18].

When genetic mutations or external factors initiate one, or more, of those mechanisms, photoreceptors death processes are activated. Which kind of intracellular pathway is, exactly, responsible in leading photoreceptors to degenerate, is still unclear. However, apoptosis is the first death-process documented to be involved in RP mouse model [19]. There is still no doubt of apoptotic events in retinal degeneration, even if many studies report conflicting evidences and show that complex crosstalk and interconnected signals are involved. It is now accepted that apoptosis of photoreceptors can occur through both a caspase-dependent and independent via [20]. Many outcomes maintain that caspases participate in cone photoreceptor

apoptosis, although neither pharmacological inhibition nor genetic manipulation of caspase cascade are able to definitely rescue photoreceptors [21]. The involvement of other proteases linked to apoptotic cell death is investigated. In particular, calpains and caspases involvement in starved-661W cells is studied, showing that calpain-mediated pathway is independent and parallel with respect to caspase activation [22]. As upstream regulators of survival or apoptosis cascade, Bcl-2 family members too are taken into consideration and become the centre of an intriguing issue. On one hand, several studies highlight the importance of Bcl-2 as anti-apoptotic molecule [23] especially, supporting it by successful Bcl-2 overexpression in rescue 661W cells from death [24]. On the other hand, some evidences show Bcl-2 failure in promote salvage signaling [25]. In any case, an increased body of evidence suggests that apoptotic mitochondrial pathway is involved in caspase-dependent or independent apoptosis of retinal cells [26]. At the same time, in a model of retinal detachment, it is showed that apoptosis of photoreceptors can occur through both exstrinsic-Fas receptor mediated and intrinsic-mitochondrial cytochrome-c dependent activation [27]. All this studies on photoreceptors apoptosis prove the involvement of a variety of woven, parallel and sometimes contradictory pathways and draw attention, as well, to non-apoptotic mechanisms [28], in particular, pointing up autophagy or its co-occurrence with apoptosis [29]. Within all the mediators able to determine photoreceptors loss or survival through regulation of the abovementioned death-salvage processes, a family of bioactive molecules, sphingolipids (SPLs), is evidenced [30]. In particular, Ceramide (Cer), Sphingosine (Sph) and Sphingosine-1-phosphate (S1P), that play an active role in regulating cell death, survival and differentiation.

1.1.3.3 Therapeutic approaches in RP

To preserve photoreceptors by RP-induced degeneration, many therapeutic strategies have been developed across the years, defining also a systematic classification depending on the degeneration stage (Fig. 1.3) [31].

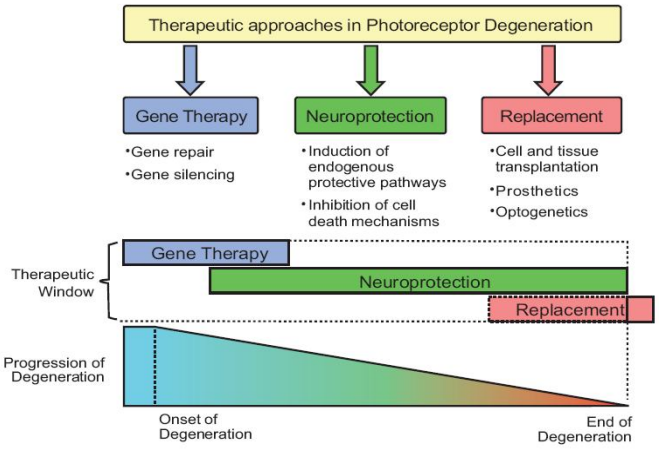

Fig. 1.3: Schematic representation of therapeutic approaches on the basis of photoreceptor degeneration stage. Original source: *Trifunović et al 2012.*

Ideally, the best way to fight a genetic disease is to correct the causative gene defect. Unfortunately this is not always feasible in RP due to, at least, two main causes: first of all, it should require an early disease diagnosis, allowing to act on genetic mutation in live cells, instead RP is recognized in patients with secondary cone degeneration already started and with all rod photoreceptors almost dead; secondly, a high efficiency to identify the gene of interest has a crucial importance and it is not easy to obtain given the wide heterogeneity of RP mutations. Nervertheless, experimental approaches to gene therapy in RP treatment have advanced in recent years. For instance, in arRP one of the most studied is the MERTK gene that encodes for the human receptor tyrosine kinase MER. MERTK located in the RPE mediates the association between these cells and the

photoreceptor outer segments. Regarding adRP, RHO and RDS/peripherin are the mutated proteins more studied. In both cases the interest is focused on a double gene therapy strategy consisting in siRNA-mediated suppression together with gene replacement [32].

Currently, many studies focus on mutation-independent ways in rescuing photoreceptors as, for example: retinal transplantation, retinal prostheses, retinal optogenetic therapy, electrical stimulation and neuroprotection through neurotrophic factors, pharmacological treatments and nutraceutical approaches. Replacement of degenerated photoreceptors with healthy transplanted tissue or cells, is a well studied practice [33]. In the last years retinal prostheses has become more and more interesting, especially with the development of new biocompatible materials and nanotechnologies [34]. The most promising device designed in this moment is Alpha-IMS, a wireless subretinal implant made up of a 1500-pixel multiphotodiode array, which combines, better than others devices, clinical availability, vision restoration potential and long-term biocompatibility. Clinical trials for this intraocular photodiode implant have already demonstrated increased patient independence by mimicking natural vision under control of eye movement [35]. Retinal optogenetic strategy, in contrast to traditional gene therapy, employ light to control genetically targeted groups of cells. It acts from the inside of the cells, using light sensors to induce ganglion or bipolar cells to become reactive to light. Once activated from light, the sensors create an electrical current that can stimulate the cell [36]. For example, channelrhodopsin-2 (ChR2), a photosensitive cation-selective channel that contains an all-*trans*-retinal chromophores, is used in a mouse model of RP. When transduced on RGCs, it restores visual responses in mice [37]. Another potential therapeutic approach is low electrical stimulation of the eye that in theory releases neurotrophic substances. Recently, transcorneal electrical stimulation (TES) in RP patients has improved the function of retinal cells, as measured by electroretinography (ERG), and the visual field

[38]. Neuroprotection can be employed in two different direction: to straighten survival stimuli and/or to stop death induction. It can consist in a board variety of treatments: neurotrophic factors [39], as NGF, BDNF, CNTF, PEDF and GDNF; nutraceutical and antioxidant agents, as, for example, vitamin A and its derivates [40], docosahexaenoic acid (DHA) [41], lutein [42] and taurine [43].

1.1.4 661W: a cone-like cell line

Many kinds of retinal cell lines are available for *in vitro* studies. Some of the most employed are: ARPE-19, human retinal pigment epithelium [44]; RGC-5, rat retinal ganglion cells [45]; R28, rat glial-neuronal cell line [46]. One in particular is suitable for the investigation of photoreceptors features and behaviours: 661W cell line. It is a cone-derived cell line, transformed by Dr. Muayyad Al-Ubaidi's group (Department of Cell Biology, University of Oklahoma Health Science Centre, Oklahoma City, U.S.). 661W were cloned from retinal tumours of transgenic mouse line expressing the SV-40 T antigen under control of the inter-photoreceptor retinal binding protein promoter (IRBP) [47]. Cells express cone but not rod specific antigens: SV40 T antigen, blue and green pigments, transducin, and cone arrestin. Immunocytochemical detection of blue and green opsins showed distribution throughout the cell, the nucleus included. However, these cells did not express rod-specific antigens, such as opsin and arrestin or rod- and cone-specific proteins such as phosducin, peripherin/RDS, and ROM1. Furthermore, the cells did not express RPE65, a cone and RPE specific protein [48]. 661W cell line is unique in its ability to respond to light stimulation and upon light stress it undergoes cell death, as showed for *in vivo* retina experiments (*www.otd.ou.edu*) [49]. Due to their easy handling and distinctive traits, 661W are widely used in ophthalmology research, especially as a model of photoreceptor degenerations subjecting them to

several kinds of stresses. In particular: light damage [49, 50], serum deprivation [22] and oxidative stress by means of several compounds, for example: hydrogen peroxide [51] [29], sodium nitro-prusside [52], sodium iodate [53] and paraquat [54]. They are also employed to investigate retinal cells inter-relations [55-58], cellular toxicity of new treatments [59], [60], and, in general, to better understand death and salvage pathway of cone photoreceptors.

1.1.4.1 Rescuing treatments on stressed 661W cells

Since 661W cone-derived cell line has been recognized as a precious *in vitro* mean for studying photoreceptors, worldwide scientific works have incremented over years. In particular, the investigation on rescuing treatments represents one of the more examined field, ranging from electrical stimulation to a whole series of different antioxidant agents and nutraceutical compounds. Electrical stimulation (ES) has been shown to promote survival on light-damaged photoreceptor through diminished microglial activation and fortified Müller cells reactive gliosis, which may have great potential in ameliorating photoreceptor damage. ES might change the activation status of microglia and Müller cells by altering transmembrane voltage-gated ion channel activity suggesting that factors of microglia or Müller cells, that can be changed by electrical fields of different strengths, must be involved in this process [61]. DHA, that is the most polyunsaturated fatty acid present in retinal neurons [62], has been demonstrated to rescue 661W cells from oxidative stress, reducing calpain activation, cytochrome c release and caspase-3 action [63]. Unoprostone isopropyl (unoprostone) is a docosanoid, known to bear neuroprotective effects and to activate large conductance Ca^{2+}-activated K^{+} (BK) channels. Unoprostone protects photoreceptors and RPE cells against oxidative- and light-induced damage by a mechanism different from antioxidant activity. In

particular, the protective effect of unoprostone is mediated by BK channel activation, probably on those existing in mitochondria, reducing the stress-induced mitochondrial damage [64]. Purple rice bran extract (PRE), derived from a coloured variety of *Oryza sativa L*. contains three anthocyanins (cyanidin 3-O-glucoside, peonidin 3-O-glucoside, and cyanidin 3-O-gentiobioside) that are supposed to be its active components. PRE inhibition of reactive oxygen species (ROS) production in visible light irradiated-661W cells was demonstrated and proposed to occur by inhibition of p38 and/or JNK activation [50]. Carnosic acid (CA), present in rosemary extract, crosses the blood–brain barrier to exert neuroprotective effects. Recently, it was found to promote survival of 661W photoreceptors and ARPE-19 cells, against H_2O_2-induced cell death. Accounting for this effect, CA induced nuclear translocation of Nrf2 and then activated transcription of phase II genes [65]. Mandal's group performs several studies on 661W evaluating the effects of antioxidant agents, especially through food-derived substances. Curcumin, a naturally occurring yellow pigment, isolated from the rhizomes of the plant *Curcuma longa*, was tested for its beneficial properties on 661W stressed with H_2O_2. Curcumin pretreated cells respond to oxidative stress activating cellular regulatory system such as NF-κB, Akt, Nrf2 and growth factors, which in turn inhibit cellular inflammatory responses and protect photoreceptors [66]. Caffeic acid phenethyl ester (CAPE), an active component of honeybee propolis, was found to activate the antioxidant gene expression pathway in H_2O_2-challenged 661W cells and in rat retinas, enhancing ERG responses [51]. Interestingly, they evidences that CAPE-altered retinal fatty acid composition probably contributed to the higher ERG responses, confirming the involvement of lipids in optimal retinal function as previously demonstrated [67].

1.2 Sphingolipids

In 1884 J.L.W. Thudichum, a german-born physician and biochemist, wrote *"A Treatise on the Chemical Constitution of Brain"*. Here he described his studies on isolation and characterization of brain constituents and, for the first time, the backbone sphingolipid: sphingosine. He chose this name such as a parallelism of this enigmatic molecule and a mysterious mythological figure: the Sphinx. Across the years, many other sphingolipids have been described until a real family of bioactive molecules have been defined [68].

1.2.1 Structure

Sphingolipids are a board and heterogeneous class of bioactive molecules, characterized by a common eighteen carbon amino-alcohol backbone, on which different biochemical modifications occur, giving rise to many metabolites. They are amphipathic molecules distinguished for relative hydrophilicity/hydrophobicity degree, strongly influencing individual intracellular localization and portability. In particular, hydrophilic region is represented by the sphingoid backbone, eventually linked to a charged headgroup, meanwhile lipidic portion is composed by N-linked acyl chains, with different numbers of carbons and insaturations. The simplest member, which actually corresponds to the common backbone, is Sph. It can undergo different modifications on C1 and C2 functional groups, in particular, acylation on C2-amino group that discriminates two big categories: sphingolipids with one or two hydrophobic chains. Different acyl chains are added through different ceramide synthases (CerS.s) that consequently generate respective Ceramides (Cer.s). Contemporarily, complexity degree can augment because of reactions on the C1-hydroxyl group. Sphingomylein (SM) arises from the binding of phosphocholine,

phosphorylation gives ceramide-1-phosphate (C1P), glycosylation, with glucose or galactose, creates the family of complex glycosphingolipids (GSLs). Finally, when acylation does not occur, phosphorylation on the hydroxyl group leads, for example, to S1P [69] (Fig. 1.4).

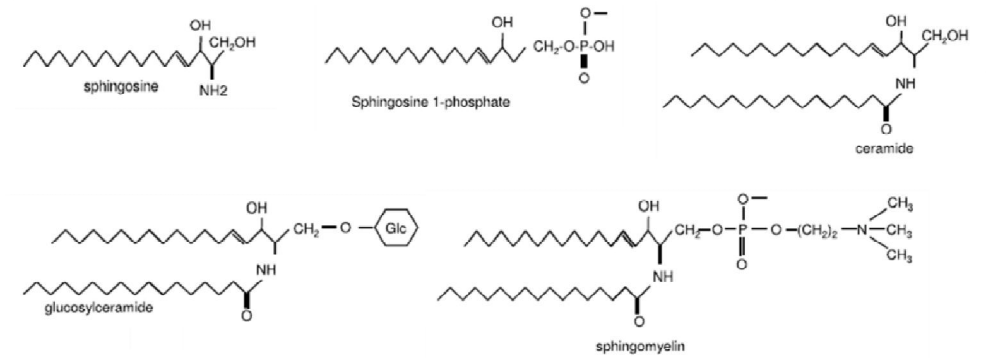

Fig. 1.4: Structures of principal sphingolipids.

Sphingolipids, as fundamental elements of lipid rafts, structurally constitute and functionally influence cellular membranes. Furthermore, they are intracellular messengers actively involved in cell functions regulation. Their heterogeneity is reflected also in their functions, insomuch as, relative species equilibrium is decisive in directing cell fate, towards death or survival pathways. The most representative example is the dualism between Cer, a death effector, and, in contrast, S1P that promotes cell proliferation and survival [68].

1.2.2 Sphingolipid metabolism

Two major pathways collaborate in the synthesis of sphingolipids: *de novo* and salvage pathway. The first one starts and ends with non-sphingolipid molecules and is characterized by an enter point, serine palmitoyl transferase (SPT), which gives rise to the first sphingoid-based member of

the family, and an exit point, sphingosine-1-phosphate lyase (SPL) that allow the irreversible degradation of S1P. *De novo* synthesis, occurring in ER, begins with SPT catalysis of cytosolic serine and palmitoyl-CoA condensation, to give 3-ketodihydrosphingosine (3-KdhSph). Since it is reduced to dihydrosphingosine, (dhSph) by 3-ketosphinganine reductase (3-KSR), and acylated by (dihydro)ceramide synthases ((dh)CerSs) with various length acyl chains, to give a wide variety of (dihydro)ceramides ((dh)Cer.s). By means of molecular oxygen and then NAPDH aid, dihydroceramide desaturase (DES) introduces a double bound in the C4-C5 position of dhCer and generates Cer [69].

Cer is now ready to eventually undergo different modifications: phosphorylation (ceramide kinase), glycosylation (glucosyl or galactosyl ceramide synthases) or condensation with a phosphocholine, deriving from phosphatidylcholine (PC), to generate SM (via sphingomyelin synthases). The latter two pools of sphingolipids represent the main source of Cer deriving from the salvage pathway, which implies its release from complex sphingolipids. Cer recycling synthesis takes place in the acidic subcellular compartments, the late endosomes and the lysosomes. Here specific exohydrolases and Acid sphingomyelinase (ASMase) degrade GSLs and SM to Cer that, in turn, is hydrolyzed by acid ceramidase (AC) to Sph able to exit the lysosomes. SM breakdown can occur also at the PM level by the action of Acid or neutral SMase depending on which side of the membrane the reaction happens and here again Cer is converted to Sph. At this point, all the Sph produced can explicate its intracellular functions or undergo to sphingosine kinases (SphK1-2) phosphorylation to generate S1P. In turn, S1P can act as second messenger, extracellular ligand or be metabolized. Two are the enzymes that can transform S1P, one is sphingosine-1-phosphate phosphatases (SPP) that regenerates Sph and the other one is sphingosine-1-phosphate lyase (SPL) that catalyzes the irreversible

degradation of S1P to phosphoethanolamine (PE, EA1P) and hexadecenal (Hex) (Fig. 1.5) [70].

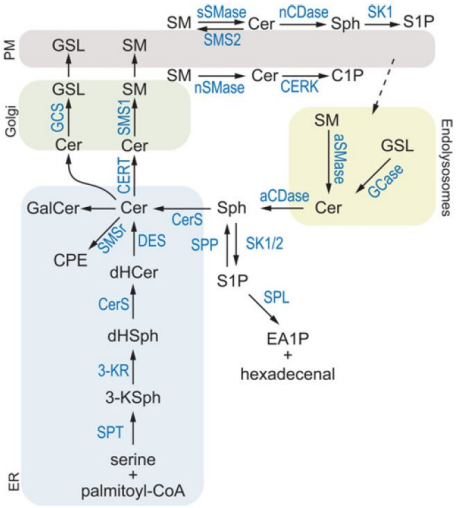

Fig. 1.5 :Summarized pathways of sphingolipid metabolisms. Original source *Mullen et al. 2012*

1.2.3 Subcellular compartmentalization

Depending on their chemical nature, sphingolipids are free to move in cytoplasmatic and extracellular spaces or are relegated into biological membranes, and linked to specific mechanisms of transport to leave their site of generation. Precisely for this reason, the roles of many sphingolipids are tightly connected with specific subcellular localization of their synthesis enzymes. In particular, their mobility is based on the number of hydrophobic chains and on the charge at neutral PH. Cer, with two aliphatic chains and neutral headgroup, can flip-flop membranes but is unable to move in cytoplasm. It reaches the Golgi apparatus through two different ways depending on which metabolite is required: by the action of transfer protein CERT, if SM generation is needed or using vesicular transport if glucosylceramide (GluCer), or in general GSLs, must be synthesized.

Vesicular transport is also involved in the mobilization of Cer hydrophobic derivate species, SM and GSLs, to the PM, from where they can be addressed to lysosomes for entering the endosomal salvage pathway. Due to more hydrophilic nature, sphingolipids with just one aliphatic chain are soluble in cytosol and can freely move among intracellular membranes. Sph, which does not present any charge, is able to flip-flop membranes meanwhile, its phosphorylated metabolite, S1P, is linked to specific transporters to pass the lipid bilayer [68]. In particular, it is demonstrated that S1P traffic is linked to ATP binding cassette (ABC) members, on one hand ABCC1 that allows its exit [71] and on the other hand cystic fibrosis transmembrane regulator (CFTR), implicated in S1P influx [72].

1.2.4 Ceramide

Cer is one of the most studied sphingolipids and represents the central point of the entire family, it is the backbone of complex members and plays a strategic role in the membrane structure and in the activation of a wide variety of intracellular pathways, depending on cell type and extracellular stimulus. Cer synthesis is catalyzed by a family of ER-localized enzymes, CerS.s, that differ in their selectivity for acyl-CoAs based on the length of the acyl chain. CerS family is composed by six members (CerS1-6) that are differently expressed in tissues and differently react to stimuli, generating the particular Cer specie requested to face the incoming situation [73].
Cer involvement in many cellular process, such as growth arrest, differentiation, apoptosis and senescence makes the regulation of its synthesis and degradation an important target in several pathologies. Depending on the length of the fatty acid added to the sphingoid base, Cer.s can be constituted by 14 to 28 carbons chains, defining several different species involved in different kind of signaling [74]. Cer.s synthesis, that can occur both through *de novo* and salvage pathway, is induced in

response to stress stimuli such as cytokines (TNF, Fas, nerve growth factor), “environmental” stresses (heat, UV radiation, hypoxia/reperfusion) and chemotherapeutic agents [75]. The intracellular pathways activated by Cer are shown to be directly linked with the ceramide-activated protein phosphatases PP1 and PP2A [76], which is demonstrated to be involved in many Cer.s-induced effects, such as dephosphorylation/inactivation of anti-apoptotic proteins including PKC, Akt and Bcl-2 [77] but also activation of apoptosis inducers as Bax [78]. Cer is also able to activate lysosomal protease cathepsin D [79], kinase suppressor of Ras as mediator of its effects on Ras, Raf, and ERKs [80] and the transcription factor NF-kB through PKC action [81].

1.2.5 Sphingosine-1-phospate

Since its recognition as an active promoter of cellular growth and survival [82], S1P gains and keeps a central position in several investigations. Nowadays, it is known that this enigmatic sphingolipid has a pivotal role in many pathologies [83] such as cancer, atherosclerosis, inflammation, neurodegeneration, cardiovascular and respiratory affections [83]. It is also involved in tissue and organs development [84], in particular in cardiogenesis [85], limb development [86], neurogenesis [87] and angiogenesis [88]. S1P signaling pathways activation is a very intriguing issue, in particular, attention is drawn on identification and especially discrimination between its effect as second intracellular messenger and/or extracellular receptors ligand [89]. In order to clarify which way is involved in different S1P effects, many studies have been developed, in particular employng pertuxiss toxin as an inhibitor of S1P-specific G protein-coupled receptors (S1PR.s). As intracellular messenger, S1P plays critical roles in calcium regulation [90] and in apoptosis inhibition [91], in particular as anti-apoptotic effector by means of many intracellular pathways. For instance,

intracellular-S1P is demonstrated to influence MAPK family members, which are known to modulate apoptosis both inducing its activation through JNK, inhibited by S1P, and, on the contrary, stopping the death process by ERK double effect on cytochrome *c* release. In fact, ERK is able to act upstream inactivating pro-apoptotic Bcl-2 family members and downstream inhibiting caspase cascade and its activation is improved by increased intracellular S1P levels [92]. SphK-S1P is also able to counteract apoptosis activating Akt, in hepatocytes [93]. Finally, it is demonstrated that intracellular synthesis of S1P is involved in NF-kB pathway activation, against TNFα effect [94].

On the other side, also S1P action through its surface receptors occupy a pivotal role in cell fate determination, similarly activating the same signaling pathways with respect to those depending on intracellular S1P. It is demonstrated that exogenous S1P can reduces Bax proteins levels in a lymphoblastoma cell line and antisense plasmids against its receptors counteract S1P-anti-apoptotic effect [95]. S1P activation of survival markers, such as ERK, are investigated in hepatoma cells stably expressing two of the five enzymes [96] and in endothelial cells where pertussis toxin blocks this ERK phosphorylation [97]. Furthermore, in this latter cellular type antisense for the first receptor attenuates S1P inhibition on Cer-induced apoptosis [98].

1.2.5.1Sphingosine-1-phosphate kinases

S1P complexity already starts in its synthesis enzyme, indeed the phosphorylation of Sph is catalyzed by SphK, which exists in two isoforms, SphK-1 and SphK-2 [99] [100]. It is well known that SphK-1 is involved in cell growth induction and apoptosis inhibition [101]. SphK-1 resides in cytoplasm and, after ERK phosphorylation, translocates to the PM [102], where its substrate, PM-associated sphingosine, is located. Generated S1P

can activate intracellular signaling or, due to the PM proximity, easily exits the cell and interacts with its cell surface receptors. SphK-2 also needs to be activated by ERK phosphorylation [103] but, saved this trait, it deeply differs from its close relative in localization, function and influence on Cer contents. Primarily, SphK-2 is found at the level of internal membranes, in particular at ER, mitochondria and nucleus and surprisingly it promotes apoptosis [104]. Which mechanism is behind its action is still unclear but, rather than to its synthesized S1P receptor interaction, it is supposed to depend on an intrinsic characteristic of the enzyme aminoacidic sequence. It is demonstrated that SphK-2 contains a 9-amino acid sequence reminiscent of the Bcl-2 homology 3 (BH3) domain present in "BH3 domain-only" proteins that, it is known to be responsible of their interaction with pro-survival Bcl-2 family members and in consequent induction of apoptosis [105]. Despite that, it has recently been demonstrated that pharmacological inhibition of SphK-2 augments cancer cells sensitivity to apoptosis [106] and its knockout abolishes preconditioning-induced tolerance in ischemia/reperfusion injury [107]. Another important difference between these two enzymes is the influence on apoptotic Cer.s intracellular amounts: SphK-1 induces a decrease of Cer.s, meanwhile SphK-2 promotes their synthesis [99].

All these outcomes open and keep alive an intriguing issue on the correlation between S1P functions and the enzyme isoform that catalyzes sphingosine phosphorylation, hence its site of creation.

1.2.5.2 Sphingosine-1-phosphate receptors

S1P-related cellular effects were associated to its function as intracellular second messenger until the discover of pertussis toxin ability in inhibiting some of its effect in fibroblasts [108]. Since then the outcome of S1P extracellular effects, mediated by surface receptors (S1PRs), were

investigated and deepened over years. In 1998, S1P was identified as a ligand of endothelial differentiation gene 1 (EDG1) product, a GPCR [109] and today the family has expanded with other four members (S1P1-5/EDG) that are accepted to be activated by extracellular S1P [110]. S1PRs add a further degree of complexity to the signaling pathways of this enigmatic sphingolipid for, at least, two reasons: their coupling to different kind of G proteins, activating respective pathways (Fig. 1.6), and their differential tissue and cell lineages expression, that can change depending on the stimulus received and/or the developmental stage. Furthermore, it is demonstrated, especially through investigation on S1P1, that S1PRs can be induced to internalize after acute agonist exposure. Two pathways of internalization are evidenced, the physiological agonist pathway which sees S1P-induced temporary internalization followed by intact receptor recycled to the PM where signaling can restart and superphysiological agonist pathway, linked to S1P-receptors potent ligands such as FTY720-P, in which ubiquitin pathway is activated and internalized receptors degrade in lysosomes [111].

S1P1/EDG1, the first discovered and the most well-studied of the family, is widely expressed in tissues and involved in T- and B- lymphocyte egress from lymphoid organs [112] also in inflammation [113] and tumorigenesis [114]. Like S1P1, S1P2/EDG5 shows a widespread expression. It is involved in increasing vascular permeability, through disruption of adherens junctions between endothelial cells [115] and upregulated by hypoxia in the retina inducing defective neovascularization and inflammatory response increasing cyclo-oxygenase-2 [116]. S1P2 plays pivotal role also in development, immunity, neural functions and cancer [117]. S1P3/EDG3, due to its coordination with S1P1 and S1P2, is barely studied alone. It is shown to play a role in immune reactions [118], in multiple sclerosis [119] and inflammation [120]. S1P4/EDG6 is highly expressed in lymphocytic and hematopoietic cells even if its role in immune modulation is still unclear

[121]. The last receptor and less investigated of the family is S15/EDG8. It shows some traits of difference against the others receptors. It is especially studied in brain and of particular interest is its differential activation in oligodendrocytes depending on their developmental stage. In fact, it mediates process retraction and impedes migration of immature cells whereas regulates survival of mature ones through Akt activation [122]. It is also involved in maintenance of the human brain endothelial barrier, in inhibiting inflammation by NF-kB activation [123] and in cancer [124].

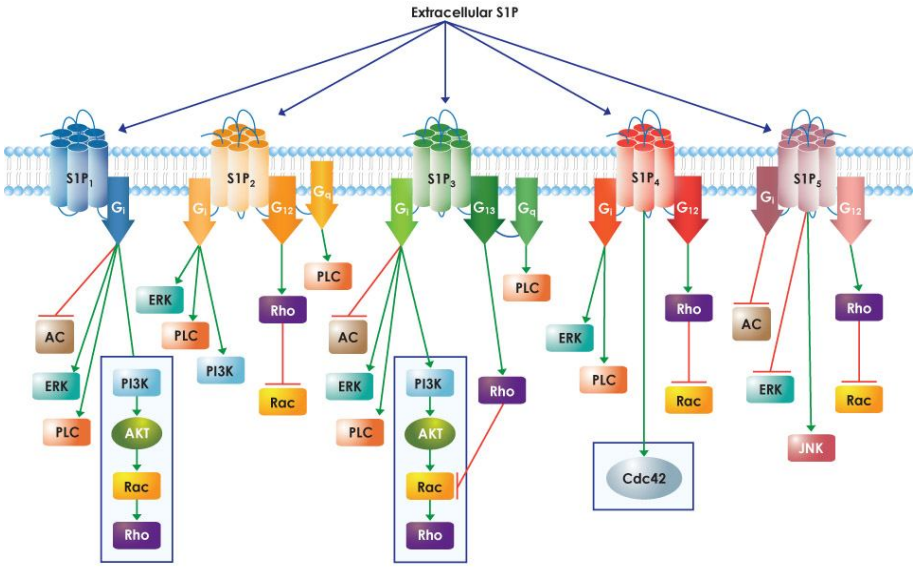

Fig. 1.6: Schematic representation of different S1PRs G-protein depending pathways. Original source: *www.caymanchem.com*

1.2.6 The entrance and the exit of the pathway: SPT and SPL

As descrived above, *de novo* sphingolipid synthesis starts and ends with no-sphingoid molecules and the two reactions, that respectively initiate the biosynthesis and terminate the catabolism of Cer, are catalyzed by two essential pyridoxal 5'-phosphate (PLP)-dependent enzymes: SPT and SPL (Fig. 1.7). They share a similar mechanism of action, which initiates with the replacement of lysine (K265 in SPT and K311 in SPL), in the Schiff base formed with the aldehyde group of PLP, with serine or S1P. The resulting external aldimine undergo to different modifications; in particular, in SPT it is subjected to a nucleophilic attack on Cα by palmitoyl-CoA thioester and, after the formation of two quinonoid intermediates and other two external aldimines, it becomes 3-KdhSph, causing the internal aldimine restoration. On the other hand, in SPL the external aldimine gives Hex after a retro-aldol cleavage, forms a quinonoid intermediate, another external aldimine and finally release PE to allow the re-formation of the resting state internal aldimine [125].

SPT is the first enzyme of the biosynthesis, localized in ER membrane-associated complex. It is composed by 3 subunits: LCB1, LCB2 and LCB3. The last one is recently characterized [126] and recognized as an isoform of LCB2. The latter two, due to their PLP-binding, are recognized as catalytic subunits, instead LCB1 relation with PLP is still to be clarified [127]. SPT expression is modulated by different stimuli [128] such as endotoxins or cytokines [129] and UVB irradiation [130].

SPL is a homo-oligomer, situated at the ER membrane with the active site exposed to the cytosol. Its activity is tightly controlled at different levels such as transcriptional, epigenetic and post-translational [131]. Due to its function as sphingolipid pathway gatekeeper and S1P level regulator it is considered an important target for several therapeutic strategies. At the moment, it is especially studied in autoimmune diseases, due to its role in

modulating lymphocytes trafficking; in fact it is widely demonstrated that SPL inhibition causes lymphopenia linked to S1P-gradient modification [132]. Furthermore, SPL expression regulation is suggested to be involved in inflammation, cancer [133], metastatic tumours [134] and protective effect against cytotoxic therapy and radiation [135].

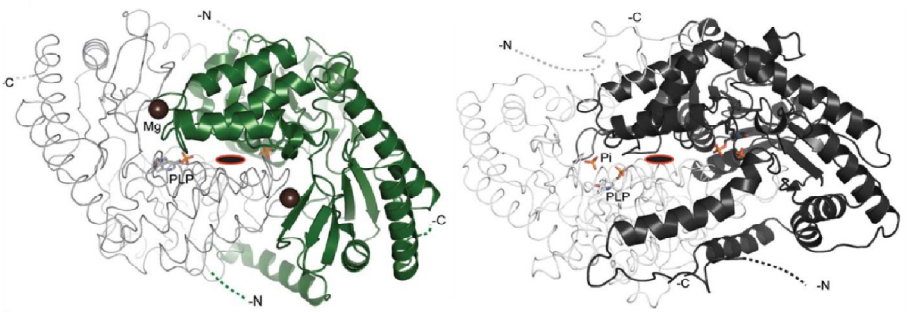

Fig. 1.7: X-ray structure of SpSPT (*Sphingomonas paucimobilis*) and StSPL (*Symbiobacterium thermophilum*). Dimeric structure of SpSPT and StSPL, represented in cartoon and ribbon with N- and C- termini indicated. PLP appears in ball-and-stick in the same color of the corresponding subunit. Original source: *Bourquin et al. 2011*

1.2.6.1 Sphingolipids pathway inhibitors: Myriocin and THI

Modification of sphingolipids levels, especially through the manipulation of critical enzymes of their biosynthetic pathway, is the basis for the study of increasing number of diseases, leading to the development of many enzymatic inhibitors or activators.

In the case of SPT, Myriocin represents a specific tool to powerfully inhibit *de novo* synthesis. Myriocin is a natural product that was firstly isolated for its antibiotic and antifungal activity from *Myriococcum albomyces* [136] and *Mycelia sterilia* (Thermozymocidin) [137], and some years later also from *Isaria sinclairi* (ISP-I) [138]. In 1995, its *in vitro* inhibition of cell growth was demonstrated to derive by SPT activity inhibition [139]. Across the years, Myriocin has been employed in a huge number of researches on: cancer

[140] [141, 142], RP [143], multiple sclerosis [144], obesity [145] atherosclerosis and cardiomyopathies [146]. Recently, its mechanism of action has been clarified: it is defined to act as a “suicide inhibitor”. Myriocin reacts with PLP to form an external aldimine that decomposes after 16 hours producing a long chain aldehyde, able to bind the active site lysine and irreversibly inactivate the enzyme [147].

SPL can be inhibited by different compounds: among these, there is 2-Acetyl-5-tetrahydroxybutyl imidazole, THI [148-150]. THI derives from ammonia caramel colour III, a food colorant belonging to the big family of ammonia caramel colours (AC) and is employed in beers, sauces and biscuits. THI biological effects were firstly evidenced in 1988, in rats, defining it as a negative modulator of circulating lymphocytes. Interestingly it was observed that deficiency of pyridoxine (Vitamin B6, whom PLP is the active form) in the diet was shown to augment THI-induced lymphopenia [151]. The same year another group analyzed THI effect on mouse and observed that THI is able to selectively induce lymphopenia also in this animal model [152]. In the following years, many studies focused on THI toxicity and on the importance of vitamin B6 in counteracting THI effect, until 1992 when a human trial, on individuals with a marginal deficit in vitamin B6, demonstrated that THI, as others ACs, did not induce any effect on blood and lympha parameters [153]. In 2005, for the first time, THI action was associated to the inhibition of SPL. Schwab’s group demonstrated that S1P abundance in lymphoid tissues of mice increased more than 100-fold after THI treatment and that it depended on SPL inhibition, especially given to the ability of vitamin B6 to tightly influence THI and other SPL inhibitors activity [154] [155]. Recently, it has been demonstrated that it has a cardioprotective effect on ischemia/reperfusion injury on murine heart [156], it abrogates eosinophilic inflammation in a mouse model of allergic rhinitis [157] and it is involved in the maintenance of energy metabolism in dystrophic mouse [158].

1.2.7 Sphingolipids in the eye

The first direct evidence of a correlation between sphingolipids and photoreceptors degeneration arrived in 2003 from Acharya's group [159]. By lowering Cer levels, they succeeded in rescueing photoreceptors in a *Drosophila* model of retinal degeneration. This outcome linked two important fields of research giving rise to many further, *in vitro* and *in vivo*, investigations. Some years later, on rat retinal neuronal cultures, C_2-Cer treatment triggered photoreceptor apoptosis, meanwhile Cer synthesis inhibition counteracted oxidative stress-induced death [160]. Similarly on 661W cells, oxidative stress, produced with sodium nitroprusside, stimulated Cer accumulation that is reduced through a SMase inhibitor [161]. Furthermore, sphingolipids result crucial also for their role as membrane structural component, in fact membrane domains enriched of sphingolipids are associated with critical photoreceptor membrane channels and manipulation of the sphingolipid pathway promotes their delocalization and dysfunction [162]. Interestingly, in a mouse model of RP, rd10, the inhibition of Cer synthesis slows retinal degeneration and preserves photoreceptors structure and function [143]. Regarding human retinal degeneration, the connection with sphingolipids was demonstrated with the finding of a mutation in a Cer kinase-like protein and arRP [17]. On the other side, S1P effects were studied in both rescue of degenerating photoreceptors and developmental retina. Apoptosis of rat retinal neuronal cells was induced by means of oxidative stress and counteracted by S1P addiction [30]. Moreover, GDNF is demonstrated to induce Sphk1 expression and translocation to the PM and, in addition, its positive effect on photoreceptors is blocked by S1P inhibition. Finally, S1P is able to increase proliferation of photoreceptor progenitors and then stimulates their differentiation [163].

2. RATIONALE

Due to their complexity, photoreceptors are the most fragile cells among those composing the retina especially due to their continuous exposition to light, high rate energy demand and constant outer segment turnover [164]. Their degeneration is the critical step of many severe retinal pathologies [18], such as RP [8]. Nevertheless, most of RP genetic mutations are related to rods, that indeed degenerates in the first stage of the disease, the following secondary cone degeneration is all along considered the major target in RP prevention [165], as also declared by Wright, in 1997: "*Keep the cones alive and some 1,5 million people worldwide will see...*" [166]. In fact, while rods death leads to night blindness, allowing an almost normal life, cones loss prevents diurnal vision and represents a tragic invalidating consequence of the pathology.

Given the critical role of sphingolipids in retinal degeneration [30] and recent evidences that Cer metabolism modulation can recover photoreceptors [143], particularly cones [167], in a murine model of RP, we investigated if both prevention of Cer formation by treating cells with Myriocin and most of all increasing the endogenous level of the pro-survival S1P, by inhibition of its degradation, can promote cones resistance to stress and save their functionality.

In order to demonstrate our hypothesis, we employed an *in vitro* model of cone-like cells and mimicked retinal degeneration stress by treating them with oxidative agents or depriving them of growth factors, the two conditions affecting cones upon rods death in RP retina.

We intend to demonstrate that not only impairment of Cer formation delays cones death but also the increase of endogenous S1P triggers a survival response that is aimed at overcoming oxidative stress. If our hypothesis is confirmed, combination of sphingolipid metabolism inhibitor can be envisaged as powerful therapy against RP retinal degeneration.

3. AIMS

This study aims at demonstrating the involvement of sphingolipids in photoreceptor degeneration, focusing on:

1) Endogenous accumulation and signaling of S1P as a mean to rescue photoreceptors from stress induced death.
2) Combination of S1P intracellular increase and Cer *de novo* synthesis inhibition to obtain additive effect on photoreceptor survival upon stress.

4. MATERIAL AND METHODS

4.1 Reagents and antibodies

H_2O_2 (hydrogen peroxide), THI (2-acetyl-4(5)-(1(R),2(S),3(R),4-tetrahydroxybutyl)-imidazole), Myriocin, fatty acid free Bovine Serum Albumin, bovine serum albumin (BSA), MTT dye, Trypan blue dye, protease inhibitor cocktail, leupeptin, Pyridoxal-5'-phosphate, L-Serine, Palmitoyl coenzyme A and Hoechst 33258 dye were purchased from Sigma-Aldrich (St. Louis, Missouri USA). Sphingosine-1-phosphate (S1P) was purcheased from Avanti Polar Lipids. Penicillin and streptomycin (Invitrogen) were purchased from Life Technologies Italia (Monza, Italy). DMEM culture media, fetal bovine serum (FBS) and the chemoluminescence system LiteAbLot were purchased from EuroClone Life Science Division (Milan, Italy). SYBR Premix Ex Taq (Tli RNaseH Plus) was purcheased from Takara Bio, Inc. (Japan), RT-qPCR primers from Eurofins Genomics (Gerrmany) and L-[^{3}H(G)]-Serine from PerkinElmer, Inc. (Massachusetts, USA)

Primary antibodies were purcheased from: p-Akt (#9271) and t-Akt (#9272) Cell Signaling; p-ERK1/2 (sc-7383), t-ERK1/2 (sc-93), Bcl-2 (sc-7382), Bax (sc-7480) and Nrf2 (sc-722) Santa Cruz; β-actin (A5316) Sigma. Horseradish peroxidase (HRP)-conjugated secondary antibody were from Jackson Laboratories (Bar Harbor, Maine, USA).

4.2 Cell cultures

4.2.1 661W

Cone-derived cell line, 661W cells, were provided by Dr. Muayyad Al-Ubaidi (Department of Cell Biology, University of Oklahoma Health Science Center, Oklahoma City, U.S.). 661W were cloned from retinal tumours of transgenic mouse line expressing the SV-40 T antigen under control of the inter-photoreceptor retinal binding protein promoter (IRBP) [47]. 661W

growth doubling time is of ~24 hours in Dulbecco's modified Eagle's medium (DMEM), supplemented with 10% fetal bovine serum (FBS) and 1% penicillin/streptomycin solution as antibiotics. They were maintained in a sterile and controlled atmosphere incubator at 5% CO_2, 95% humidity at 37 °C. Experiments were performed in 96 ($3x10^3$ cells in 0,2 ml), 6 ($2,5x10^5$ cells in 3 ml) multiwell plates and 100 mm Petri dishes ($8x10^5$ cells in 6 ml) starting treatments after about 24 hours, however when cells reached a 60%-70% confluence.

4.2.2 MDA-MB-231

Human breast cancer cell line MDA-MB-231, from America Type Culture Collection (ATCC), Rockville, MD, USA, was chosen as source of Serine-Palmitoyl Transferase (SPT) enzyme. Cells were maintained at 5% CO_2, 95% humidity at 37 °C in DMEM, supplemented with 10% FBS and 1% penicillin/streptomycin solution as antibiotics. Cells were seeded in 150mm Petri dishes ($3x10^6$ cells in 24 ml) and left to grow for at least 3 days, however until 80-90% confluence was reached, before collected them for microsomal membranes fraction extraction, due to the localization of the studied enzyme at this level.

4.3 Cells treatments

661W cells were stressed through hydrogen peroxide (H_2O_2 1mM) and serum starvation (1% FBS DMEM). They were pre or cotreated with the following compound: S1P (1µM and 100nM), solubilized in a methanol:water (95:5) solution, dried through a stream of dry nitrogen and stored according to the Avanti Polar Lipids protocol. Before use, S1P was resuspended in sterile fatty acid free Bovine Serum Albumin (BSA, 4 mg/ml), to make a 125 µM S1P solution and incubated for 30 minutes at 37°C, sonicated and vortexed occasionally. THI (75 µM) and Myriocin (10 µM) were both solved in dimethyl sulfoxide (DMSO).

The same procedure was followed prior to all assays: cells were seeded and left to grown for about 24 hours in 10% FBS/1% penicillin/streptomycin DMEM. Before treatments, the media was replaced with 10% or 1% FBS DMEM, depending on the kind of stress, always without antibiotics, and appropriate compound was added. At proper time point, they were collected and processed according to different assays.

4.4 3-(4,5-dimetiltiazol-2-il)-2,5difeniltetrazolio bromide (MTT) assay

Cell growth curve was performed, evaluating cell proliferation by MTT assay at 12, 24 and 48 hours after stress. Cells were seeded in 96-well tissue culture plates at $3x10^4$ cells/well. At every time point, 20 µl of MTT solution (5 mg/ml) were added in each well and 661W cells were incubated, in darkness, at 37°C for 4 h. Media was removed, 100 µl of DMSO was added and the optical density (O.D.) was measured at 540 nm with a microplate reader (Sunrise Tecan microplate reader). Identical concentrations were tested in six-repetitions and the assay performed at least three times. Results are expressed as proliferation index fold change with respect to time zero (T0), against time.

4.5 Trypan blue dye exclusion test

Trypan blue assay was used to evaluate the number of viable cells after treatments. 661W cells were seeded in tissue culture Petri dishes (100mm) at $8x10^5$ cells/Petri, treated and after 12 hours, counting was evaluated in experimental and control groups. For that, cells were detached using 0.25% trypsin, for 5 minutes at 37°C, collected and resuspended in 2 ml of Phosphate buffered saline (PBS) solution, 90 µl aliquots of this cell suspension were added to 10 µl of 0,4% Trypan blue dye (1:10). Next, live and dead cells were counted using Bürker chamber under a MoticAE31

optical inverted microscope. Live and dead cells were reported as both number of cells and percentages over the control.

4.6 Western blotting

Protein expression levels were analyzed by Western blotting. Cells, seeded at $8x10^5$ in each tissue culture Petri dishes (100 mm), were treated and, after 12 hours, collected by scraping on ice in cold PBS-EDTA buffer, containing protease inhibitor cocktail. Then samples were centrifuged at 800g for 5 minutes at 4 °C, supernatants were discarded and pellets resuspended in 80 ul of the same buffer. A 15 ul aliquot, for every sample, was used for total protein quantification (µg/ul), through Bradford method [168]. The remaining suspension was added with Laemmli solution [169], boiled for 8 min and stored at -20°C. Proteins (15ug) were separated by SDS-PAGE with different concentrations acrylamide gels, depending on investigated protein size (10% for ERKs, Akt and Nrf2, 15% for Bcl2 and Bax. Proteins were transferred onto a nitrocellulose membrane with and unspecific binding sites were blocked by one hour of 5% dry skimmed milk in tris-buffered saline (TBS) containing 0.1% Tween-20 (TBS-T) For immunoblotting, membranes were incubated at 4°C overnight with primary antibodies: anti p-ERK1/2 (1:500 in TBS-T-3% BSA), anti t-ERK1/2 (1:500 in TBS-T-3% BSA), anti p-Akt (1:1000 in TBS-T-3% BSA), anti t-Akt (1:1000 in TBS-T-3% BSA), anti Bcl-2 (1:200 in TBS-T), anti Bax (1:200 in TBS-T) and anti Nrf2 (1:1000 in TBS-T). β-actin levels (anti β-actin 1:2000 in TBS-T-3% BSA) were quantified for Nrf2 amounts normalization and as loading control for all others markers analyzed as protein levels ratio: ERK1/2 and Akt (phosphorylated on total form), Bcl-2 and Bax (Bcl-2, anti-apoptotic, on Bax, pro-apoptotic, marker). Membranes were incubated with the proper horseradish peroxidise (HRP) conjugated secondary antibody diluted 1:10000 in TBS-T-5% dry skimmed milk or TBS-T, depending on the

primary antibody. Bands detection was obtained by chemoluminescence and X-ray film exposure. Specific bands intensity was quantified by Gel Doc 2000, with Quantity one software (Bio-rad gel doc system, Chemidoc XRS). Levels of proteins were expressed in different ways, see respective figure captains for clarifications.

4.7 Liquid chromatography-tandem mass spectrometry (LC–MS) analysis

In order to measure sphingolipids intracellular amounts, cells were collected and total protein fractions were quantified following the protocol applied for Western blotting analyses. The obtained cellular pellets were lyophilized or directly frozen at -80 °C. Sphingolipids extracts from untreated and treated cells, fortified with internal standards (N-dodecanoylsphingosine, N-dodecanoylglucosylsphingosine, N-dodecanoylsphingosyl phosphorylcholine, C17-sphinganine (0.2 nmol each) and C17-sphinganine-1-phosphate (0,1 nmol), were prepared and analyzed as reported [170]. S1P amount was measured without adding internal standards.

4.8 Terminal deoxynucleotidyl transferase dUTP nick end labelling (TUNEL) assay

Apoptosis degree was evaluated by means of TUNEL test, trypsinized cells were washed in 1 ml cold PBS and centrifuged 5 min at 1000 rpm at 4° C. The pellet was resuspended in 500 µl of 4% cold buffered formalin for 30 min, washed in PBS, centrifuged (1000 rpm, 5 minutes, 4 °C), resuspended in 50 µl PBS and stratified on slides (Superfrost Plus-Menzel Gmbh and CoKG, Braunschweg, Germany). After drying at room temperature, slides were maintained at –20 °C until use. Apoptosis was determined by the TdT assay (In situ Cell Death Detection Kit, TMR Roche Diagnostics,

Mannheim, Germany) in an inverted fluorescence microscope (40x magnification) Axiovert25 CFL (Zeiss, Göttingen, Germany) equipped for the detection of rhodamine (filter set 15, excitation band pass 546 nm, emission low-pass 590 nm). Nuclei were stained with the karyophilic dye Hoechst 33258 (250 ng/ul) for 3 minutes at room temperature in the dark, followed by rinsing twice in PBS and coverslipping. Slides were examined using a filter for Hoechst staining (filter set 02, excitation band pass 365 nm, emission low-pass 420 nm). Images were acquired by a digital camera (DS-2MV; Nikon, Tokyo, Japan) and the number of TdT-labeled nuclei counted (8-10 random fields in a blinded procedure). Results are expressed as number of TdT-labeled nuclei/total nuclei.

4.9 Ferric reducing antioxidant power (FRAP) assay

Cellular supernatants were separated from pellets and used to perform FRAP assay according to the method of Benzie & Strain [171] with minor modifications. Briefly, to prepare the FRAP solution, 100 ml of acetate buffer 300 mM, adjusted to PH 3.6 with acetic acid, were mixed with 10 ml of ferric chloride hexahydrate 20 mM dissolved in distilled water and 10 ml of 2,4,6-tris(2-pyridyl)-s-triazine 10 mM dissolved in HCl 40 mM. 100 µl of sample were added to 3 ml of a freshly prepared FRAP solution in glass test tubes in triplicate and the absorbance was measured at 593 nm after 5 minutes of incubation at 37 °C against a blank of acetate buffer. Aqueous solutions of $FeSO_4 \cdot 7H_2O$ (100–1000 µM) were used for the calibration and the results were expressed as FRAP value (µM Fe (II)) of the samples [172].

4.10 Real-time PCR (RT-qPCR)

To evaluate the influence of treatments on mRNA synthesis, real-time PCR was performed. 661W cells were seeded in 6-well tissue culture plates at $2{,}5x10^5$ cells/well and treated. After 12 hours, total RNA was extracted with miRNeasy Mini Kit (Qiagen) according to the manufacturer's instructions. RNA was quantified by fluorometry with Qubit (Life Technologies Italia) and about 1 ug of total RNA was reverse transcribed in cDNA. The reaction was performed in a final volume of 20 µl starting with an incubation of 45 minutes at 37 °C and continuing for others 45 minutes at 42 °C to induce the degradation of eventual secondary RNA structures. RT-q Polymerase chain reaction amplification of the respective genes were performed with the SYBR Premix Ex Taq and set up in a total volume of 20 µl, with 200nM forward and reverse primers through the SYBR Green system according to the protocol. For the amplification, the following primers were used (5′->3′orientation). Primer's sequences of target genes, heme oxygenase-1 (HO-1) [51] and S1PRs (S1P1, S1P2, S1P3, S1P4 and S1P5) [173], were obtained from published studies.

HO-1	forward TCTATCGTGCTCGCATGAAC
	reverse CTGTCTGTGAGGGACTCTGG
S1P1	forward AAATGCCCCAACGGAGACTCTG
	reverse TTGCTGCGGCTAAATTCCATGC
S1P2	forward CCCAACTCCGGGACATAGA
	reverse ACAGCCAGTGGTTGGTTTTG
S1P3	forward TCAGTGGTTCATCATGCTGG
	reverse CAGGTCTTCCTTGACCTTCG
S1P4	forward AAGACCAGCCGTGTGTATGG
	reverse TCAGCACGGTGTTGAGTAGC
S1P5	forward GCCTGGTGCCTACTGCTACAG

	reverse	CCTCCGTCGCTGGCTATTTCC
GAPDH	forward	AACTTTGGCATTGTGGAAGG
	reverse	ACACATTGGGGGTAGGAACA

Specificity of PCR products was confirmed by analysis of a melting curve. Real-time PCR amplifications were performed on a CFX96 Real-Time System (Bio-Rad). Amplification of the house-keeping gene GAPDH (Glyceraldehyde 3-phosphate dehydrogenase) was performed to standardize the amount of sample RNA. Relative quantification of gene expression was achieved using the 2-DeltaDeltaCt method as previously described [174].

4.11 Serine palmitoyltransferase (SPT) activity assay

Microsomal membranes fraction was collected through MDA-MB-231 homogenization in a specific extraction buffer (Hepes PH 7.4 25 mM, EGTA PH 7.8 5 mM, NaF 50 mM, leupeptin 10 µg/ml and tripsin inhibitor 10 µg/ml) and centrifugation at 4070 rpm for 10 minutes at 4 °C. After Bradford protein assay, the enzymatic assay was performed incubating 300 µg of total proteins at 37 °C for 30 minutes in the reacting buffer (Hepes PH 8.3 100 mM, EDTA PH 7.4 2.5 mM and DTT 5 mM) containing Pyridoxal-5'-phosphate 50 µM as enzymatic cofactor and L-[^{3}H(G)]-Serine (1 mM, 2 µCi specific activity 26 Ci/mmol), L-Serine (1 mM) and Palmitoyl coenzyme A (200 µM) as substrates. Counts per minute (CPM) were measured with β-counter (Packard Tri-Carb Liquid Scintillation Analyzer, model 2900TR) after washing three times the organic phase with bi-distilled water, dividing the two phases (hydrophilic and organic) with various centrifugations, drying up the samples overnight at 39 °C and resuspending them in scintillation cocktail. Results are expressed as percentage of enzymatic activity with respect to the control (DMSO) ± Standard Deviation, assuming

boiled enzyme as zero. Only for most interesting compounds, IC50 was obtained through a concentration-response curve performed calculating the enzymatic activity ± Standard Deviation at different concentrations.

4.12 Statistical analysis

Data on 661W cells are provided as means ± SEM. Statistic significance was evaluated for all data, choosing the best method depending on the number of analyzed groups: paired two-tailed Student's *t*-test for two-group comparison and one-way analysis of variance (ANOVA) for multiple-group comparison, with Bonferroni post hoc test when $P<0.05$. Only results with $P<0.05$ were considered statistically significant. All statistical computations were carried out with InStat 3.01 (GraphPad Software, San Diego, California, USA). Western blot and TUNEL images are the most representative of at least three independent experiments.

5. RESULTS

5.1 H_2O_2 and serum deprivation inhibit proliferation and viability in cone photoreceptors

661W cells were challenged through 1mM H_2O_2 or starved in 1% serum medium (serum deprivation, SD) for 12, 24 and 48 hours and cellular proliferation was assessed by MTT assay. Oxidative stress induced 30% inhibition of cellular proliferation within the first 12 hours of treatment, whereas SD induced 50% proliferation inhibition in 48 hours (Fig. 5.1A and B). Both treatments induced a three folds increase of cell death, measured by Trypan blue assay, after 12 hours (Fig. 5.1C).

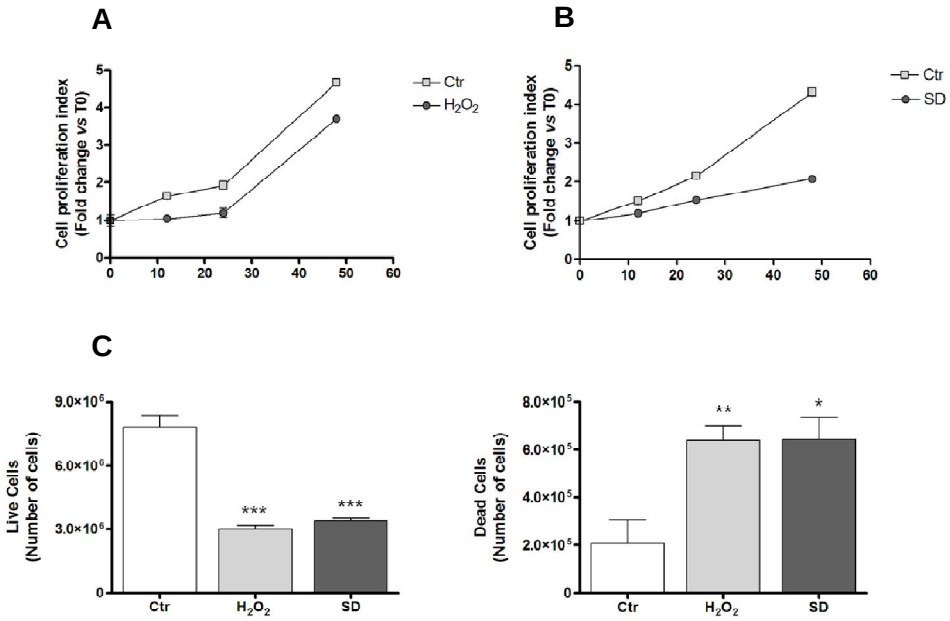

Fig. 5.1: Oxidative stress and serum deprivation affect *in vitro* cone photoreceptors proliferation and viability. Cells were treated with 1mM H_2O_2 or starved with 1% FBS DMEM for 12, 24 and 48 hours. A-B) Cell proliferation was evaluated by MTT assay. Data are expressed as fold change *vs* time zero (T0) against time. C) Photoreceptors viability was assessed through Trypan blue exclusion assay after 12 hours of stresses. The number of live and dead cells was showed in graphs. Data are obtained from three experiments and values are expressed as average ± SEM. Significance was analyzed through ANOVA followed by Bonferroni multiple comparisons post test, when $P<0.05$. *$P < 0.05$, **$P < 0.01$, ***$P < 0.001$, n.s. not significant. SD: Serum deprivation.

In order to identify the mechanism underpinning cell arrest and death, we studied the involvement of key mediators of survival/death signaling. Stress activated kinases ERK1 and 2 are known to be phosphorylated to promote survival. In H_2O_2 or SD 12 hours treated 661W cells, ERKs were significantly dephosphorylated, in agreement to the above reported effect on cell death induction (Fig. 5.2A). Akt phosphorylation on Ser 473, was shown to be enhanced under acute, but sub-lethal oxidative stress in retinal pigment epithelial cells [175]. 661W cells, treated with 1mM H_2O_2 or SD for 12 hours exhibited an increase of Akt phosphorylation on Ser 473: six folds and four folds respectively for H_2O_2 and SD (Fig. 5.2B).

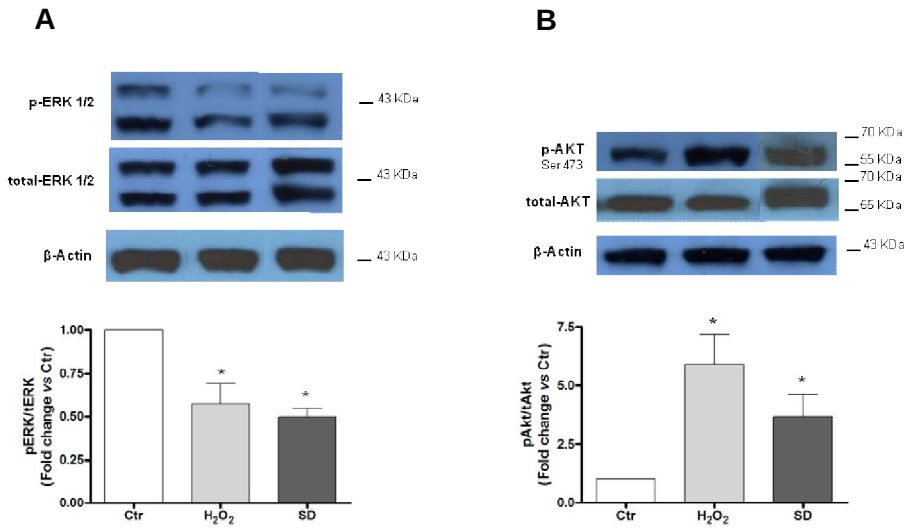

Fig. 5.2: Oxidative stress and serum deprivation modulate ERK1/2 and Akt phosphorylation. Cells were treated with 1mM H_2O_2 or starved with 1% FBS DMEM for 12 hours. A-B) The effect of 12 hours of 1mM H_2O_2 or 1% SD treatment was studied on ERKs and Akt phosphorylation. Cell lysates were resolved by SDS-PAGE and immunoblotted with antibodies for p-ERKs, t-ERKs (44 and 42 kDa), p-Akt and t-Akt (60 kDa). Value of densitometry quantification of phosphorylated forms were normalized on corresponding total forms and the ratio was expressed as fold change vs control (Ctr), untreated cells; β-actin (43 kDa) was showed as loading control. Western blot images are the most significant among those quantified. Data are obtained from three experiments and values are expressed as average ± SEM. Significance was analyzed through ANOVA followed by Bonferroni multiple comparisons post test, when $P<0.05$. *$P < 0.05$, **$P < 0.01$, ***$P < 0.001$, n.s. not significant. SD: Serum deprivation.

5.2 THI rescues photoreceptors from both stresses, without affecting unchallenged cells.

THI is an inhibitor of SPL, leading to S1P cell accumulation. S1P is a pro-survival inducer which was shown to counteract Cer induced cell death when its intracellular levels raise above the baseline. In order to rescue photoreceptors from stress induced cell death, we treated 661W cells with 75 μM THI, either 2 hours before H_2O_2-stimulus or in cotreatment with SD. We monitored cellular proliferation at 12, 24 and 48 hours, and observed a slight but significant recovery in THI cell survival, visible already at 12 hours and more evident over time (Fig. 5.3A and B). After 12 hours of treatments, we observed that the percentage of live cells augmented almost of 25% and the number of dead cells lowered almost three folds in both stresses (Fig. 5.3C and D).

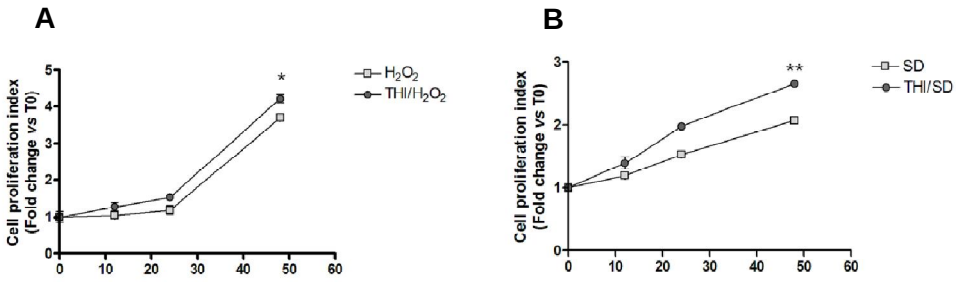

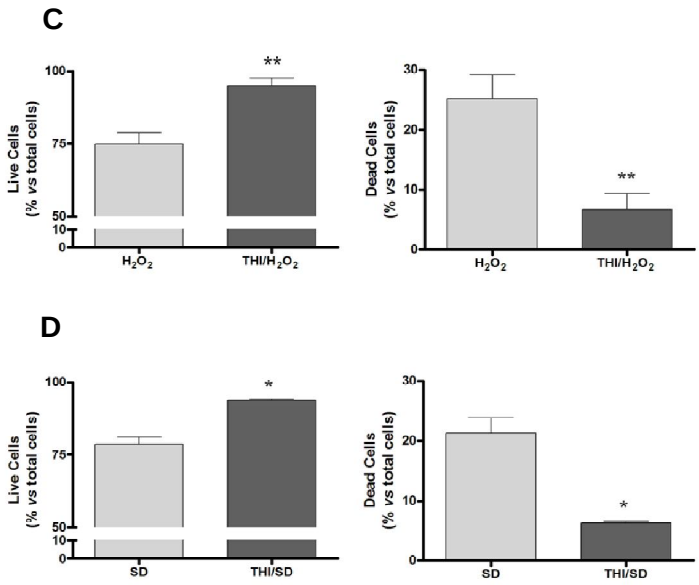

Fig. 5.3: THI attenuates stresses effects on 661W cells. 75μM THI was added to cells, two hours before 1mM H_2O_2 and directly with 1% FBS DMEM (SD). Cells were analyzed after 12, 24 and 48 hours from stress induction. A-B) Cell proliferation was evaluated by MTT assay. Data are expressed as fold change *vs* time zero (T0), against time. C-D) Photoreceptors viability, in presence of THI, was assessed by Trypan blue exclusion assay after 12 hours of stress. Percentages of live and dead cells were calculated considering total cells as 100%. Data are obtained from three independent experiments and values are expressed as average ± SEM. Significance was analyzed through Student t-test. *P < 0.05, **P < 0.01, ***P < 0.001, n.s. not significant. SD: Serum deprivation

Once again, we investigated a possible involvement of ERKs and Akt pathways: THI always antagonized death-stimuli, by increasing activation of ERK by 1.5 folds against H_2O_2 and two folds against SD (Fig. 5.4A) and by inducing a 35-40% reduction of Ser473 Akt phosphorylation (Fig. 5.4B).

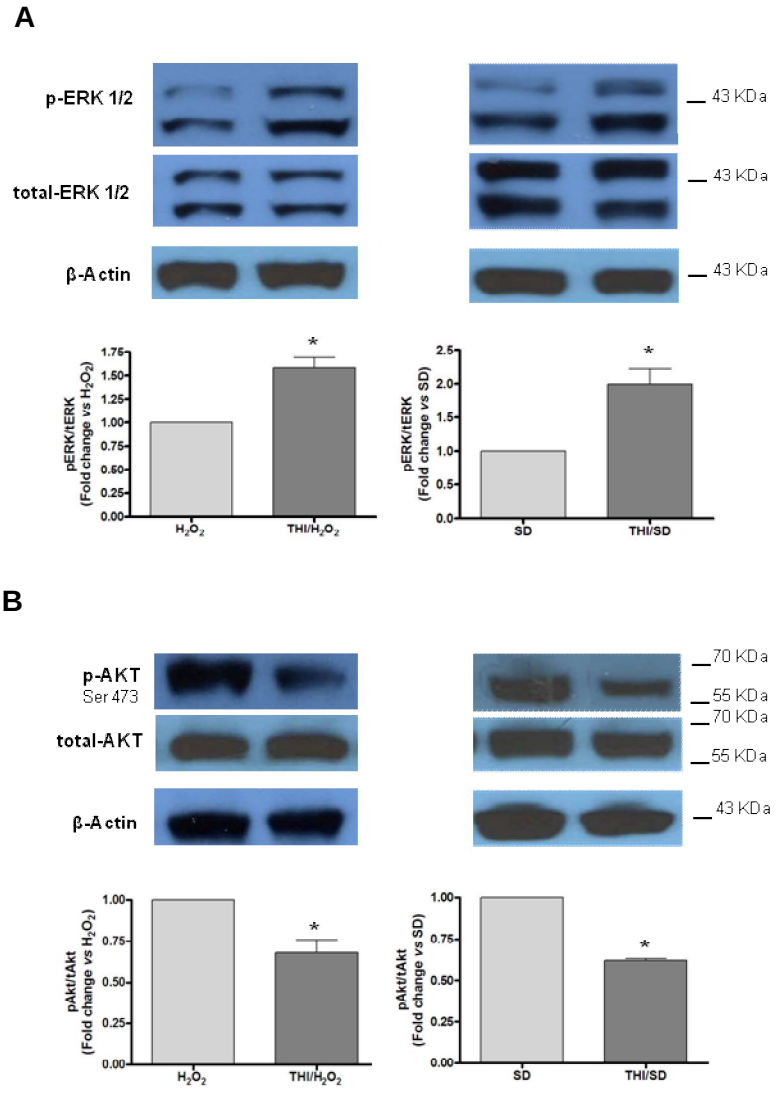

Fig. 5.4: THI counteracts stresses effect on ERK1/2 an Akt phosphorylation. 75μM THI was added to cells, two hours before 1mM H_2O_2 and directly with 1% FBS DMEM. THI rescue action was studied on ERKs and Akt phosphorylation. A-B) Cell lysates were resolved by SDS-PAGE and immunoblotted with antibodies for p-ERKs, t-ERKs (44 and 42 kDa), p-Akt and t-Akt (60 kDa). Value of densitometry quantification of phosphorylated forms were normalized on corresponding total forms and the ratio was expressed as fold change vs stress (H_2O_2 or SD); β-actin was showed as loading control. Western blot images are the most significant among those quantified. Data are obtained from three independent experiments and values are expressed as average ± SEM. Significance was analyzed through Student t-test. *P < 0.05, **P < 0.01, ***P < 0.001, n.s. not significant. SD: Serum deprivation

We also evaluated THI influence on unstressed photoreceptor viability, showing that the enzymatic inhibitor did have no significant effects on survival per se (no change in live and dead cells ratio: Fig. 5.5).

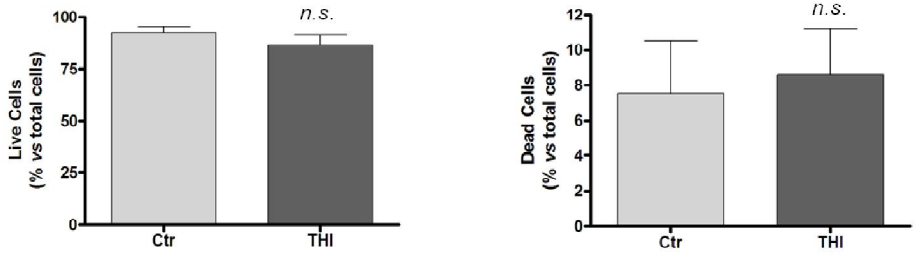

Fig. 5.5: THI does not influence photoreceptors viability. Percentages of live and dead cells were evaluated after 12 hours of 75μM THI, considering total cells as 100%. Data are obtained from three independent experiments and values are expressed as average ± SEM. Significance was analyzed through Student t-test, when P<0.05. *P < 0.05, **P < 0.01, ***P < 0.001, n.s. not significant.

5.3 H_2O_2 and SD influence Cer contents in different ways

We investigated how stress influenced Cer total and single species amount, differing for length and saturation of the amide linked acyl chain. Liquid-chromatography coupled to mass-spectrometry analysis (LC-MS) was performed on total lipids extracts of 661W cells, after 12 hours of stress. H_2O_2 did not significantly change total Cer but elicited its action modulating single species amount. On one hand, it significantly augmented long-chains Cer.s: 1.5 folds N-C_{16} acyl chain, 2.5 folds N-C_{18} acyl chain, 3 folds N-C_{20} acyl chain species; on the other hand, a 50% decrease was showed for N-C_{24} acyl chain Cer, the very long chains species analyzed (Fig. 5.6A).

We also studied SD effect on Cer species discovering that it never caused Cer amounts raise but instead it decreased them. This is in accordance with the starvation shut down of any synthesis activity and/or autophagy promotion. Significant decrease was observed only for the total Cer.s, reduced of about 30% with respect to the control (Fig. 5.6B).

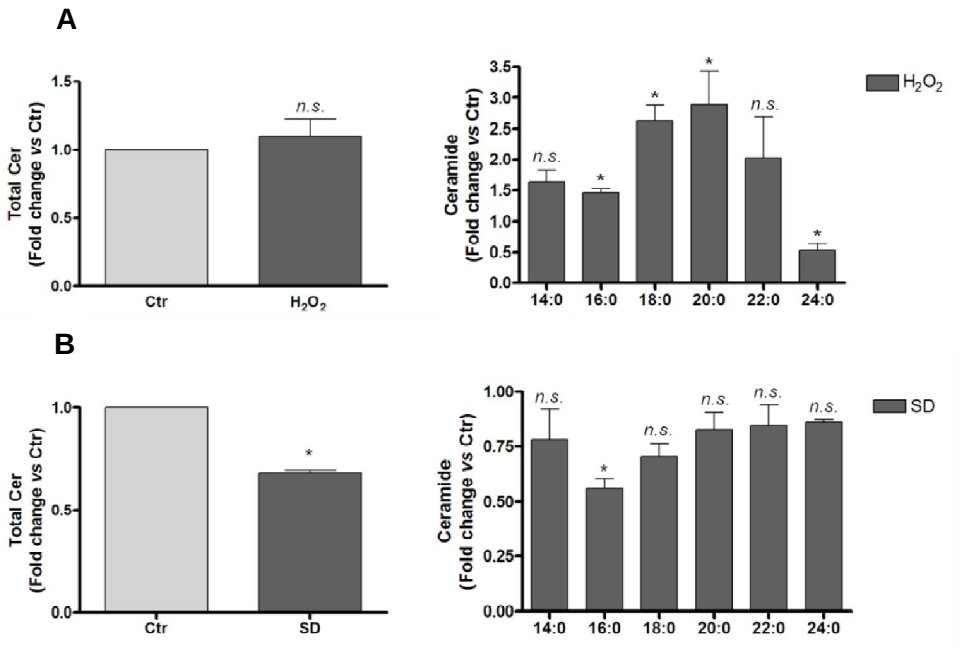

Fig. 5.6: Oxidative stress and serum deprivation change cellular Cer.s amount. Cells were stressed with 1mM H_2O_2 and 1% FBS DMEM for 12 hours. A-B) Lipid extracts were analyzed for the quantification of total and six single Cer species (from N-C_{14} to N-C_{24} acyl chain Cer.s) by means of LC-MS. Cer amounts (picomoles) were normalized on milligrams of proteins and showed values were expressed as fold change *vs* control (Ctr), untreated cells. Data are obtained from three experiments and values are expressed as average ± SEM. Significance was analyzed through Student t-test. *P < 0.05, **P < 0.01, ***P < 0.001, n.s. not significant. SD: serum deprivation

5.4 THI lowers Cer contents in H_2O_2-challenged photoreceptors

Given the antithetic role of Cer and S1P, we focused our study on ceramide-inducing oxidative stress, since SD did not alter Cer level. Two hours of 75μM THI pretreatment, followed by 1mM H_2O_2 for 12 hours, reduced Cer both as total level (25%) and almost all the single species. Regarding shorter-chain members, reductions were: 30-35% for N-C_{14} acyl chain and N-C_{18} acyl chain and 50% for N-C_{20} acyl chain species. THI significantly acted also on longer Cer, lowering of 30-35% both N-C_{22} acyl chain and N-C_{24} acyl chain elements (Fig. 5.7).

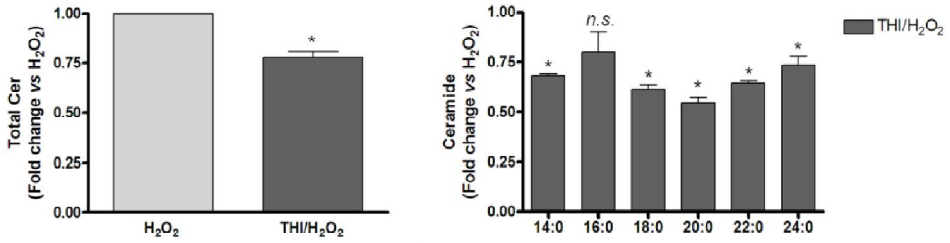

Fig. 5.7: THI counteracts Cer H_2O_2-induced raise. Cells were pretreated with THI for two hours and stressed with 1mM H_2O_2. After 12 hours, lipid extracts were analyzed for the quantification of total and six different Cer.s (from N-C_{14} to N-C_{24} acyl chain Cer.s) by means of LC-MS. Cer amounts (picomoles) were normalized on milligrams of proteins and showed values were expressed as fold change *vs* H_2O_2. Data are obtained from three experiments and values are expressed as average ± SEM. Significance was analyzed through Student t-test. *P < 0.05, **P < 0.01, ***P < 0.001, n.s. not significant.

5.5 THI and H_2O_2 oppositely modulate S1P intracellular content

Due to THI function as inhibitor of S1PL, we investigated S1P amounts changes, through LC-MS measurement, on treated and untreated 661W cells and we observed low but significant modulation induced both by THI and H_2O_2. In particular, THI promotes the accumulation of S1P with respect to the control (Fig. 5.8A) and, conversely oxidative stress induces a 40% decrease of its amount (Fig. 5.8B). Finally, we were not able to determine a significant change when 661W cells are pretreated with the inhibitor and then stressed with H_2O_2 (Fig. 5.8C).

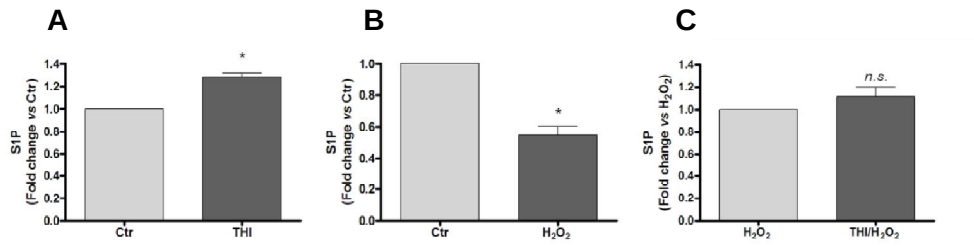

Fig. 5.8: THI and H_2O_2 act on S1P amounts. Cells were pretreated with THI for two hours and stressed with 1mM H_2O_2. After 12 hours, lipid extracts were analyzed for the quantification of S1P by means of LC-MS. S1P amounts were normalized on milligrams of proteins and showed values were expressed as fold change against Ctr or H_2O_2 depending on the treatment evaluated: A) THI *vs* Ctr; B) H_2O_2 *vs* Ctr and C) THI/H_2O_2 *vs* H_2O_2. Data are obtained from three experiments and values are expressed as average ± SEM. Significance was analyzed through Student t-test. *P < 0.05, **P < 0.01, ***P < 0.001, n.s. not significant.

5.6 Oxidative stress increases apoptosis in 661W cells and activates Nrf2/HO-1 pathway

To study the outcome of oxidative stress and above reported signaling in cone like cell line, we investigated on apoptosis in Cer accumulating cells after H_2O_2 treatment. First, we performed TUNEL assay after 12 hours of 1mM H_2O_2 and obtained a 50% apoptosis above the baseline control cells, as evidenced in the corresponding immunofluorescence images below (Fig. 5.9A). Next we investigated apoptosis mechanism and analyzed the cytosolic presence of the pro-survival Bcl-2 and the pro-apoptotic Bax. The relation between these two proteins, both Bcl-2 family members, is crucial in cell fate determination, indeed, while Bax-Bax homodimer induces apoptosis, Bcl-2-Bax heterodimer promotes survival signals [176]. The shift of their ratio expresses an ongoing apoptosis path, dominant Bcl-2 saves cells from death, whereas major Bax expression triggers to apoptosis. We performed Western blotting to quantify Bcl-2 and Bax. The ratio Bcl-2/Bax, observed under H_2O_2 treatment was decreased about four folds with respect to the control (Fig. 5.9B).

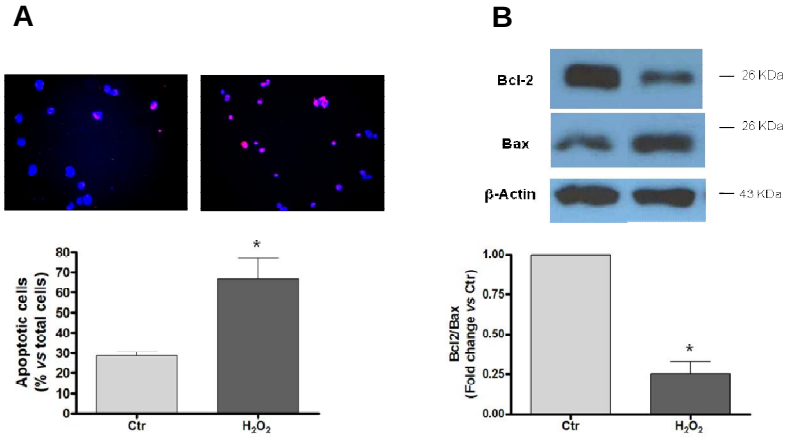

Fig. 5.9: Oxidative stress induces apoptosis in photoreceptors. Cells were stressed with 1mM H_2O_2 for 12 hours. A) TUNEL-assay was performed to estimate the apoptosis degree. Images show TdT-positive nuclei labeled with rhodamine (red) and counterstained-Hoechst 33258 nuclei (blue). Apoptotic cells percentage was expressed as average number of TdT-positive nuclei on total amount of nuclei present. B) Apoptosis was also investigated by quantification of Bcl-2/Bax ratio. Cell lysates were resolved by SDS-PAGE and immunoblotted with antibodies for Bcl-2 (26 kDa) and Bax (23 kDa). The two proteins were quantified by densitometry and their ratio was calculated and reported in graph as fold change *vs* control (Ctr) untreated cells; β-actin (43kDa) was showed as loading control. Western blot images are the most significant among those quantified. Data are obtained from three experiments, values are expressed as average ± SEM. Significance was analyzed through Student t-test. *P < 0.05, **P < 0.01, ***P < 0.001, n.s. not significant.

H_2O_2 toxicity is exerted by ROS induction within the cell. Intracellular survival response consists in the formation of antioxidant molecules that are released in colture medium. Their concentration can be evaluated by means of FRAP (Ferric reducing antioxidant power) test, which measures their ferric reducing power. H_2O_2-treated 661W cells revealed a 40% decrease of antioxidant-intrinsic power, after 12 hours treatment (Fig. 5.10A). A key player of the antioxidant survival response is Nrf2. This latter is a transcriptional factor whose ubiquitination and proteolysis is impaired under oxidative stress leading to its transcriptional activation of ARE-dependent genes, among which ROS defence related proteins, such as HO-1 [177]. To better understand the ongoing pathway, we investigated Nrf2/HO-1 activation in 661W cells treated with 1mM H_2O_2. We performed a Western blotting quantifing Nrf2 at 12 hours and we noticed an initial increase of Nrf2 activation (Fig. 5.10B).

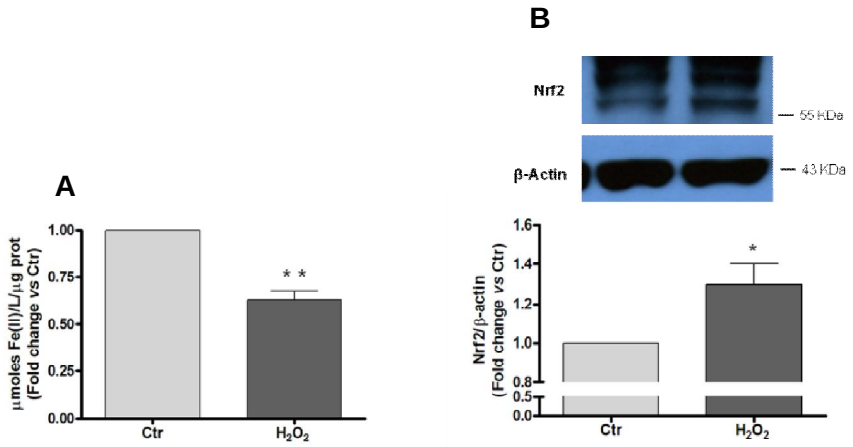

Fig. 5.10: Oxidative stress induced Nrf2 expression in 661W. Cells were stressed with 1mM H_2O_2 for 12 hours. A) Antioxidant compounds release in supernatant was analyzed by the FRAP test and expressed in FRAP value (µmoles Fe(II)/µg proteins) as fold change *vs* control (Ctr), untreated cells. B) Activation of antioxidant molecular pathways was studied through the densitometric analysis of Nrf2 Western blotting bands (57kDa) from total cell lysates. Values were normalized on the corresponding β-actin (43kDa) and expressed as fold change *vs* control (Ctr) untreated cells. Data are obtained from three experiments, values are expressed as average ± SEM. Significance was analyzed through Student t-test. *P < 0.05, **P < 0.01, ***P < 0.001, n.s. not significant.

Finally, we analyzed HO-1 mRNA content by Real-Time PCR (RT-qPCR) at 12, 24 and 48 hours and a potent induction (ten folds increase) of HO-1 mRNA transcription was observed at the first time point. HO-1 transcript level decreases over time, side by side with cell demise (Fig 5.11).

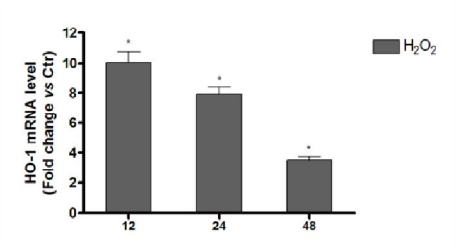

Fig. 5.11: Oxidative stress strongly upregulates HO-1 transcript expression at early time points. 661W were stressed with 1mM H_2O_2 for 12, 24 and 48 hours and mRNA expression level of HO-1 was analyzed by RT-qPCR. Data were normalized on GAPDH housekeeping gene and expressed as fold change vs control (Ctr), untreated cells. Data are obtained from three experiments, values are expressed as average ± SEM. Significance was analyzed through Student t-test. *P < 0.05, **P < 0.01, ***P < 0.001, n.s. not significant.

5.7 THI counteracts H_2O_2-induced apoptosis, eliciting its antioxidant action through additional activation of Nrf2 pathway

To study the potential of THI and S1P accumulation and signaling in reducing oxidative-stress induced death in cone-like cells, we pretreated 661W cells with THI 75 μM for two hours and then treated them with H_2O_2 1mM for 12 hours and studied cell death by TUNEL assay. TUNEL-stained cells reached 70% in H_2O_2 and decreased to 30% in THI/H_2O_2, as shown in the immunofluorescence images below (Fig. 5.12A). When looking at the molecular pathway involved, the Bcl-2/Bax ratio resulted increased by three folds in THI-protected cells, with respect to H_2O_2-traeted cells (Fig. 5.12B).

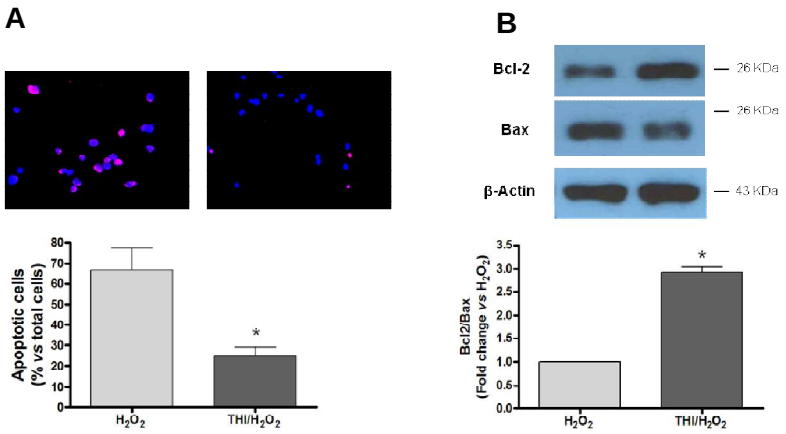

Fig. 5.12: THI reduces photoreceptors apoptosis degree. THI Cells were pretreated with THI for two hours and stressed with 1mM H_2O_2 for 12 hours. A) TUNEL-assay was performed to estimate the apoptosis degree. Images show TdT-positive nuclei labeled with rhodamine (red) and counterstained-Hoechst 33258 nuclei (blue). Apoptotic cells percentage was expressed as average number of TdT-positive nuclei on total amount of nuclei present. B) Apoptosis was also investigated by quantification of Bcl-2/Bax ratio. Cell lysates were resolved by SDS-PAGE and immunoblotted with antibodies for Bcl-2 (26 kDa) and Bax (23 kDa). Ratio of densitometry quantifications were calculated and reported in graph as fold change *vs* H_2O_2, β-actin (43 kDa) was showed as loading control. Western blot images are the most significant among those quantified. Data are obtained from three experiments, values are expressed as average ± SEM. Significance was analyzed through Student t-test. *P < 0.05, **P < 0.01, ***P < 0.001, n.s. not significant.

Antioxidant-induced activity of THI was observed by FRAP analysis and appeared to be two folds augmented against stressed 661W, in collected-colture media (Fig 5.13A). We also investigated if THI protection was due to modulation of endogenous survival response. Indeed we observed a further increase in Nrf2 accumulation and activation in THI/H_2O_2-treated cells with respect to 12 hours H_2O_2-stressed photoreceptors (Fig 5.13B).

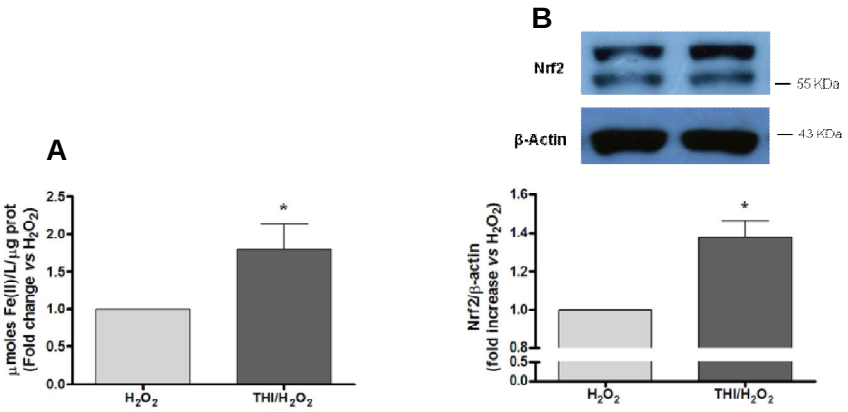

Fig. 5.13: THI increases antioxidant-intrinsic power of photoreceptors and potentiates Nrf2 expression. Cells were pretreated with THI for two hours and stressed with 1mM H_2O_2 for 12 hours A) Antioxidant compounds release in supernatant was analyzed by the FRAP test and expressed in FRAP value (µmoles Fe(II)/µg proteins) as fold change *vs* H_2O_2. B) Activation of antioxidant molecular pathways was studied through the densitometric analysis of Nrf2 protein bands (57kDa). Values were normalized on the corresponding β-actin (43kDa) and expressed as fold change *vs* H_2O_2. Data are obtained from three experiments, values are expressed as average ± SEM. Significance was analyzed through Student t-test. *P < 0.05, **P < 0.01, ***P < 0.001, n.s. not significant.

Correspondingly, the antioxidant survival response was enhanced at 12 hours and, in addition, it was prolonged and improved as showed by the maintenance of high levels of HO-1 transcript up to 48 hours (Fig 5.14). This observation is in accordance with THI recover from death, starting at 12 hours and within the same time frame (see above, Fig. 5.3A).

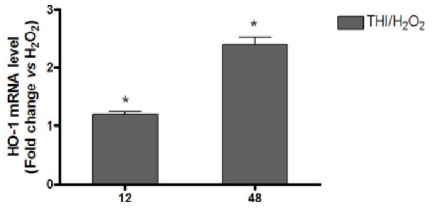

Fig. 5.14: THI enhances HO-1 transcription, over time, against oxidative stress. Cells were pretreated with THI for two hours, stressed with 1mM H_2O_2 for 12 and 48 hours and mRNA expression level of HO-1 was analyzed by RT-qPCR and data were normalized on GAPDH housekeeping gene and expressed as fold change *vs* H_2O_2. Data are obtained from three experiments, values are expressed as average ± SEM. Significance was analyzed through Student t-test. *P < 0.05, **P < 0.01, ***P < 0.001, n.s. not significant.

5.8 S1P receptors expression in 661W cells

Due to the scarcity of studies on S1P signaling in 661W cells, we could not find any evidence of S1P-receptors expression in this cell line. S1P is known to act as endogenous signaling mediator but also to be secreted by specialized pump and act in a paracrine fashion, via GPCR receptors engagement. Therefore we analyzed the expression, by RT-qPCR, of the known five isoforms of S1PRs in 661W cell line. We showed that the entire family of S1PRs was expressed in our cells, pointing out an almost decreasing linearity from the first to the last member (Fig. 5.15).

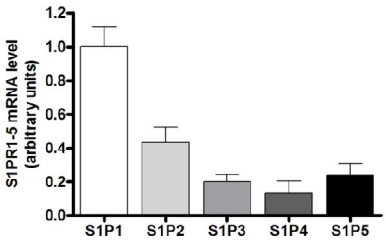

Fig. 5.15: S1PR1-5 in photoreceptors. mRNA expression levels of all five S1PRs were analyzed by RT-qPCR, data were normalized to the endogenous GAPDH control gene and expressed as fold change vs the first receptor (S1PR1). Data are obtained from three experiments, values are expressed as average ± SEM.

5.9 THI and H_2O_2 influence S1P receptors transcripts expression

To better understand the role and the power of THI on stressed photoreceptors, we evaluated the mRNA transcript modulation on 661W cells in presence of THI and H_2O_2-treatment. After THI stimulation the expression of the last two receptors, S1P4 and S1P5, was strongly upregulated, reaching about a four folds increase, instead of S1P1, S1P2 and S1P3 that did not sense THI-effect (Fig. 5.16).

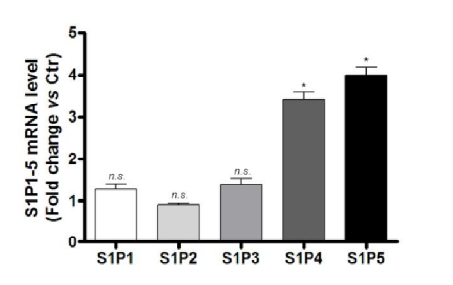

Fig. 5.16: THI modulates S1P4 and S1P5 mRNA expression. Cells were treated with 75μM THI. mRNA expression levels of all five S1PRs was analyzed by RT-qPCR, data were normalized on GAPDH housekeeping gene and expressed as fold change *vs* control (Ctr), untreated cells. Data are obtained from three experiments, values are expressed as average ± SEM. Significance was analyzed through Student t-test. *P < 0.05, **P < 0.01, ***P < 0.001, n.s. not significant.

On the contrary, 12 hours of oxidative stress produced a significant decrease of S1P3, S1P4 and S1P5 mRNA, in particular it halved their amounts. H_2O_2 did not have the same effect on S1P1 and S1P2 transcript expression and especially it did not affect S1P2 mRNA at all (Fig. 5.17)

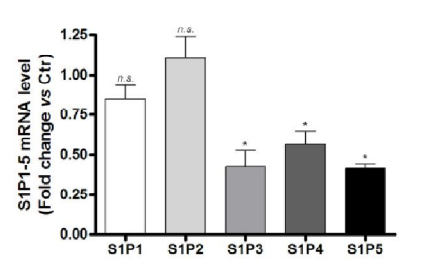

Fig. 5.17: Oxidative stress affects S1P3, S1P4 and S1P5 mRNA expression. Cells were challenged with 1mM H_2O_2 for 12 hours. mRNA expression levels of all five S1PRs was analyzed by RT-qPCR, data were normalized on GAPDH housekeeping gene and expressed as fold change *vs* control (Ctr), unstressed cells. Data are obtained from three experiments, values are expressed as average ± SEM. Significance was analyzed through Student t-test. *P < 0.05, **P < 0.01, ***P < 0.001, n.s. not significant.

We observed that THI cotreatment did not significantly change S1P2 and S1P3 transcript amounts with respect to that of oxidative stressed cells. Meanwhile, S1P1 mRNA was weakly incremented, S1P4 and S1P5 mRNA were highly upregulated showing a four folds and an eight folds increase respectively (Fig. 5.18).

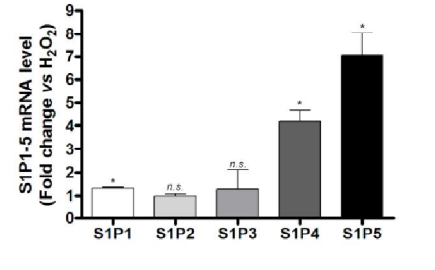

Fig. 5.18: THI counteracts H_2O_2 effect on S1P1, S1P4 and S1P5 mRNA expression. Cells were pretreated with THI for two hours and then with 1mM H_2O_2 for 12 hours. mRNA expression levels of all five S1PRs was analyzed by RT-qPCR, data were normalized on GAPDH housekeeping gene and expressed as fold change *vs* H_2O_2. Data are obtained from three experiments, values are expressed as average ± SEM. Significance was analyzed through Student t-test. *P < 0.05, **P < 0.01, ***P < 0.001, n.s. not significant.

5.10 Extracellular S1P rescues photoreceptors from oxidative stress

Due to the above reported evidence of THI modulation of S1P1-5 receptors expression, we decided to investigate a possible paracrine action for the endogenously produced S1P in 661W rescue.

Therefore we analyzed the effect of exogenously administered S1P. Cells were pretreated with 1μM and 100nM S1P for 1 hour, before oxidative stimulus, cell proliferation was assessed after 12, 24 and 48 hours through MTT assay. First we observed a strict dependence of receptor signaling on agonist concentration, as expected for GPCRs regulated by agonist inactivation. Whereas 1μM S1P did not trigger protection against stress (Fig. 5.19A), S1P low concentration, 100 nM, reduced H_2O_2 induced arrest of proliferation, measured by MTT, at 12, 24 and 48 hours (Fig. 5.19B). To analyze cell viability, Trypan blue exclusion assay was performed after 1 hour of 100nM S1P pretreatment and 12 hours of oxidative stress, percentage of live and dead cells was determined with respect to total cell number. The number of alive cells increased 25% and, at the same time, dead cells were diminished about three folds (Fig. 5.19C).

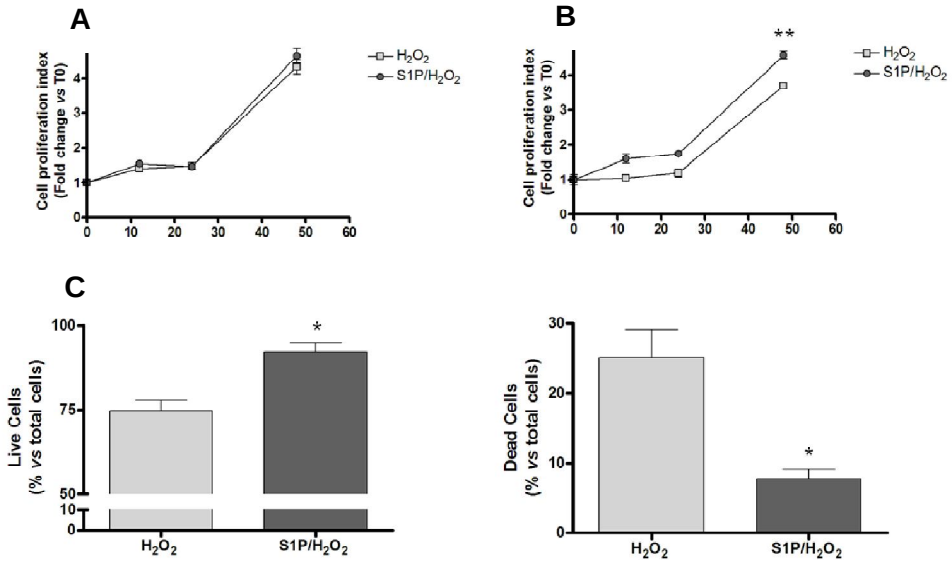

Fig. 5.19: Extracellular S1P counteracts H_2O_2 action. 1µM (A) and 100nM (B) S1P was added to cells, one hour before 1mM H_2O_2 and cells were analyzed after 12, 24 and 48 hours from stress. Cell proliferation was evaluated by MTT assay. Data are expressed as fold change *vs* time zero (T0), against time. C) Photoreceptors viability, in presence of S1P, was assessed with Trypan blue exclusion assay after 12 hours of stress. Percentages of live and dead cells were calculated considering total cells as 100%. Data are obtained from three experiments and values are expressed as average ± SEM. Significance was analyzed through Student t-test. *P < 0.05, **P < 0.01, ***P < 0.001, n.s. not significant.

To assess a possible antioxidant-induced power of extracellular S1P against H_2O_2, FRAP assay was performed in collected-colture media. FRAP value obtained from S1P pretreated cells was significantly higher (two folds) in comparison with those from stressed photoreceptors (Fig. 5.20).

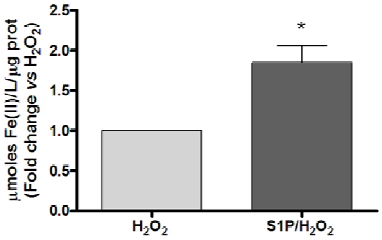

Fig. 5.20: Exogenous S1P improves antioxidant-intrinsic photoreceptors power. 100nM S1P was added to cells, one hour before 1mM H_2O_2 and cells were analyzed after 12 hours from stress. Antioxidant compounds release in supernatant was analyzed by the FRAP test and expressed in FRAP value (µmoles Fe(II)/µg proteins) as fold change *vs* H_2O_2. Data are obtained from three experiments and values are expressed as average ± SEM. Significance was analyzed through Student t-test. *P < 0.05, **P < 0.01, ***P < 0.001, n.s. not significant.

5.11 Myriocin strongly affects Cer amounts as single treatment and with THI, both in unstressed and stressed cells

S1P derives from the rupture of Cer amide linkage and the release of sphingosine and fatty acid. Sphingosine is immediately phosphorylated to avoid toxicity. Thus S1P may derive either from ceramide neo-synthesis or from ceramide release from sphingomyelin hydrolysis. In order to trace a possible contribution of ceramide *de novo* synthesis under oxidative stress, 661W cells were pretreated with Myriocin, an inhibitor targeting the first and rate limiting step of ceramide biosynthesis pathway.

THI did not affect significantly Cer amounts except for the shorter specie studied: N-C_{14} acyl chain. Myriocin, in single treatment but also in combination with THI, reduced four times total ceramides and downregulated all studied species: 50% reduction in N-C_{14} acyl chain and N-C_{18} acyl chain species, 60% in N-C_{20} acyl chain specie, 70% in N-C_{16} acyl chain and N-C_{22} acyl chain species and 90% in N-C_{24} acyl chain specie (Fig. 5.21)

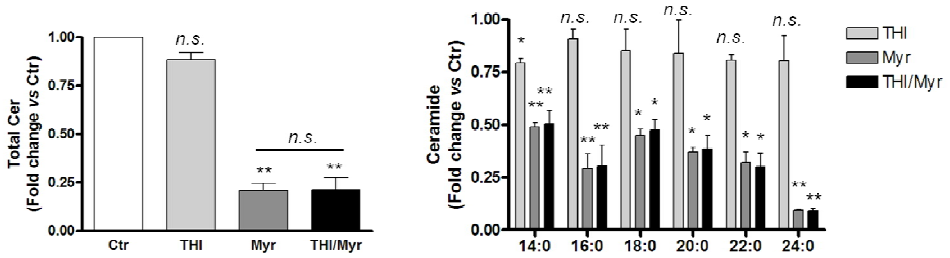

Fig. 5.21: Myriocin drastically decreases Cer.s amounts. 10μM Myriocin and 75μM THI were added to cells. After 12 hours, lipid extracts were analyzed for the quantification of total and six single Cer species (from N-C14 to N-C24 acyl chain Cer.s) by means of LC-MS. Cer.s amounts (picomoles) were normalized on milligrams of proteins and values were expressed as fold change *vs* control (Ctr), unstressed cells. Data are obtained from three experiments and expressed as average ± SEM. Significance was analyzed through Student t-test. *P < 0.05, **P < 0.01, ***P < 0.001, n.s. not significant.

Pretreatment of 661W with Myriocin, before oxidative stress with H_2O_2, induced a 50% reduction in Cer.s, affecting all fatty acyl species. As expected, THI combination with Myriocin did not alter Cer.s profile with respect to Myriocin only (Fig. 5.22).

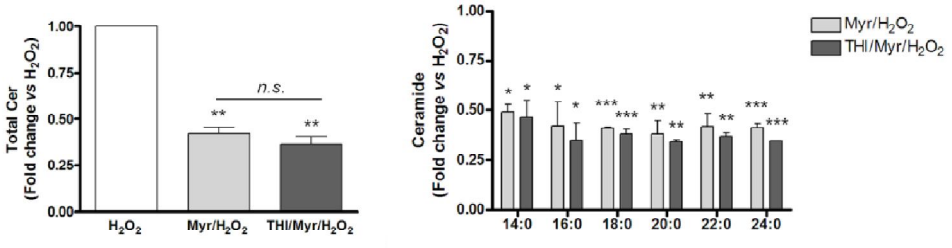

Fig. 5.22: Myriocin antagonises H_2O_2-induced increase of Cer.s.. 10μM Myriocin and 75μM THI were added to cells, five and two hours before 1mM H_2O_2. After 12 hours, lipid extracts were analyzed for the quantification of total and six single Cer species (from N-C14 to N-C24 acyl chain Cer.s) by means of LC-MS. Cer.s amounts (picomoles) were normalized on milligrams of proteins and values were expressed as fold change *vs* H_2O_2. Data are obtained from three experiments and expressed as average ± SEM. Significance was analyzed through Student t-test. *P < 0.05, **P < 0.01, ***P < 0.001, n.s. not significant.

5.12 Myriocin and Myriocin-THI treatments counteract oxidative stress effect on photoreceptors.

In order to evaluate Myriocin effects on 661W cells, Trypan blue exclusion assay was performed, pretreatment with 10μM Myriocin for five hours before the addition of H_2O_2, or THI 75μM (2 hours) and then oxidative stress was carried on for other 12 hours. 75% inhibition of survival was obtained with H_2O_2 only (Fig. 5.23). Myriocin and Myriocin/THI treatments insured a recover of survival up to 90% and 95%, respectively, after oxidative stress. Accordingly, dead cells ratio lowered almost five times with both treatments.

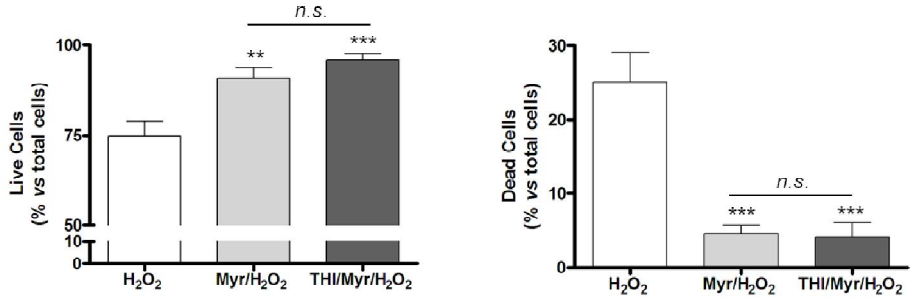

Fig. 5.23: Myriocin and Myriocin-THI recover 661W cells viability from oxidative stress.. 10μM Myriocin and 75μM THI was added to cells, five and two hours before 1mM H_2O_2. Cells were analyzed after 12 hours. Photoreceptors viability, in presence of inhibitors, was assessed with Trypan blue exclusion assay. Percentages of live and dead cells were calculated considering total cells as 100%. Data are obtained from three experiments and values are expressed as average ± SEM. Significance was analyzed through ANOVA followed by Bonferroni multiple comparisons, when $P<0.05$. *$P < 0.05$, **$P < 0.01$, ***$P < 0.001$, n.s. not significant.

Antioxidant-induced effect of Myriocin and THI on H_2O_2 stress was evaluated by means of FRAP assay, in colture media. Both Myriocin and Myriocin/THI induced two folds increase in antioxidant factors release with respect to H_2O_2 (Fig. 5.24).

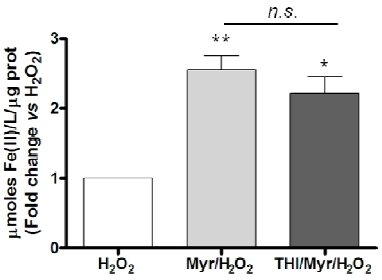

Fig. 5.24: Myriocin and Myriocin-THI have antioxidant-induced activity against H_2O_2. 10µM Myriocin and 75µM THI were added to cells, five and two hours before 1mM H_2O_2. Antioxidant compounds release in supernatant was analyzed by the FRAP test and expressed in FRAP value (µmoles Fe(II)/µg proteins) as fold change *vs* H_2O_2. Data are obtained from three experiments and values are expressed as average ± SEM. Significance was analyzed through Student t-test. *P < 0.05, **P < 0.01, ***P < 0.001, n.s. not significant.

5.13 New synthetic compounds: SPT inhibitors

In order to characterize new compounds with the same activity of Myriocin in inhibiting SPT, the rate limiting enzyme of the ceramide synthesis pathway, a number of compounds have been synthesized as potential inhibitors. Due to SPT internal membranes localization, enzymatic activity was evaluated in enriched fractions of microsomal membranes obtained from MDA-MB 231 cells. This cell line was chosen for its high proliferation rate and also basing on our laboratory experience, however it was previously employed to study SPT *in vitro* activity [178]. The enzyme inhibitory activity of 30 new compounds, developed from different backbone structures, was tested *in vitro*. We considered Myriocin incubation with microsomal membranes-SPT extract as positive control and DMSO incubation (vehicle of each compound) as 100% of SPT activity. At first, inhibitors were screened at a fixed concentration of 50μM, only the most promising molecules were selected and tested at scalar concentration to determine their IC50 value.

From the first step screening, we found three active inhibitors on SPT: DC9, DC14 and DC80, that lowered the percentage of SPT activity to 5.68%, 12.58% and 29.90% respectively. Therefore, we measured their IC50, resulting in: DC9 17.71μM, DC14 19.42μM and DC80 40.41μM (Tab. 5.1).

Compound name	**SPT activity ± SD (% *vs* DMSO)**
A7	139.35 ± 21.73
A9	56.17 ± 3.24
DC6	177.91 ± 8.59
DC9	**5.68 ± 2.15**
DC10	81.65 ± 10.81
DC11	157.63 ± 1.77
DC12	153.83 ± 10.50
DC13D	87.92 ± 5.63
DC14	**12.58 ± 2.08**
DC20A	102.26 ± 14.38
DC21A	94.85 ± 5.93
DC25A	98.26 ± 4.68
DC46B	118.85 ± 3.02
DC50A	116.76 ± 11.27
DC63C	103.47 ± 4.64
DC70	108.45 ± 1.25
DC71	105.11 ± 5.01
DC74	123.16 ± 6.40
DC79	92.8 ± 3.49
DC80	**29.9 ± 9.46**
DC81	65.58 ± 2.23
DC82	58.9 ± 5.35
PR1	92.22 ± 3.61
PR2	106.99 ± 4.19
RB6	104.68 ± 8.66
RB7	77.83 ± 4.79
RB8	42.69 ± 1.74
RB17	106.56 ±0.36
RB19	59.6 ± 3.94
RB20	94.24 ± 6.80

Compound name	**IC50 ± SD (μM)**
DC9	17.71 ± 1.00
DC14	19.42 ± 4.98
DC80	40.41 ± 4.77

Tab. 5.1: Comparative analysis of the 30 compounds tested for SPT. Synthetic compounds were tested on SPT activity at 50μM and their inhibition power was indicated as percentage of SPT activity considering DMSO incubation as 100%. Three of them, that showed a remaining percentage of enzymatic activity under 30%, were analyzed to determine their IC50. Data are obtained from three experiments and values are expressed as average ± SD

.

6. DISCUSSION

This study aims at demonstrating the involvement of sphingolipids in photoreceptor death, suggesting the manipulation of this signaling molecules as potential therapeutic targets in retinal diseases. In particular, we worked on a stressed cone-like cell line as a model of cone photoreceptors degeneration. In RP, cones photoreceptors degeneration is secondary to rods damages and it occurs mainly as bystander effect. This makes this process suitable for therapeutic approaches aimed at reducing the potency of stress insults on viable cones.
In spite of rods degeneration and considering the importance of cones preservation to allow minimal daily vision, the purpose of our study is to increase intracellular S1P concentration through the inhibition of SPL, the enzyme responsible for one of the two degradation pathway.

The cone-like cell line, 661W, is a unique *in vitro* model of photoreceptors, derived from mouse retinal tumours [47]. In the intent to investigate the possibility to activate salvage pathways of these photoreceptors, we subjected 661W cells to two different kind of stress: oxidative stress by means of H_2O_2 and ischemia-like condition throughout serum deprivation (SD). Due to their different nature, these two stresses produced distinct effects, evidenced in cell proliferation measurement over time. In Fig.5.1A and B, we showed, on one side, how H_2O_2 effect was pronounced causing apoptosis in a large part of the population whereas a small fraction of cells remained viable and proliferating, proportionally to the control rate. On the other side, we observed that SD progressively reduced cellular proliferation rate over time. Hence the two stress are sensed differently and may activate diverse stress responses: oxidative stress can be considered an acute and intense stimulus, partially overcome by a small number of resistant and growing cells; SD fails to select resistant cells, and slowly affects the entire population because of continuous lack of necessary nutrients, such as growth factors.

First of all, we considered cellular viability at the 12 hours time point (Fig. 5.1C). Both stresses resulted in a strong decrease of live cells and in a parallel augment of death at this early time point. To understand the intracellular pathways involved, we chose two well known proteins with pivotal role in cells proliferation and survival, ERKs and Akt. The ERK/MAPK pathway activation is often linked to proliferation and survival in both *in vitro* and *in vivo* models [179]. Particularly ERKs activation in rat retina was associated to protection against light injury [180], as well as in 661W cell colture under short stimulation with H_2O_2 (30 minutes). Although an initial survival response is triggered by the cells, if stress is sustained in time, cell demise will finally follow [181]. Accordingly, we observed that 12 hours of H_2O_2 treatment or SD cause cell death and ERKs dephosphorylation (Fig. 5.2A). Another important player in survival responses is the kinase Akt/PKB, whose activity is modulated during pathological situations [182] such as retinal degeneration, indeed Akt activation was demonstrated to rescue rat retinal neurons from light-induced apoptosis [183]. Cotter's group showed, in 661W, that serum deprivation induced a rapid but detectable burst of H_2O_2, activating survival pathways and promoting Akt phosphorylation, at Thr408 [184]. Years later the same group demonstrated that bFGF administration to 661W enhanced ROS production and again Akt phosphorylation occurred, even if on Ser473 [185], the same phosphorylation was documented in H_2O_2- stressed RPE [175]. Another group demonstrated that, in a different stress and cellular model, the site of Akt phosphorylation changed depending on the severity of the stress: Ser473 phosphorylation was associated to an early stress meanwhile Thr408 corresponded to intense and prolonged stress [186]. Our results confirmed that oxidative stress, as well as SD, induced Akt activation that resulted in Ser473 phosphorylation (Fig. 5.2B). In our model Akt activation persisted with respect to that on ERK suggesting a potential regulation of Akt in switching off of the ERK pathway.

S1P is a well-know anti-apoptotic sphingolipid able to induce cell survival, proliferation and differentiation in several cell lines and tissues [83]. Furthermore, S1P was recognized to participate in photoreceptors protection against oxidative stress [163]. In order to investigate a potential role of S1P in rescue 661W from death-induced stimuli, we treated cells with THI, SPL inhibitor, at the aim of increasing the endogenous amount of S1P. Inhibitory effect of this compound is mainly used in studies on autoimmune disorders. Due to its ability to accumulate S1P, THI induces its gradient deregulation that consequently leads to lower levels of circulating peripheral lymphocytes [150]. In our study we treated cells with THI 2 hours prior to H_2O_2 (1mM) and contemporarily with SD. THI pretreatment was able to reduce stresses inhibition of proliferation from 12 up to 48 hours of treatment (Fig. 5.3A and B). Moreover THI exerted a protective effect on cell death, increasing the number of viable cells in both starved and H_2O_2 stressed samples (Fig. 5.3C and D). To analyze the correlation between intracellular S1P and survival intracellular signaling [187], the activation state of ERK and Akt was analyzed under THI action. In both cases the inhibitor was able to counteract stress effects, on one side by inducing the activation of switched-off ERK 1 and 2 (Fig. 5.4A), on the other side by decreasing stress-induced phosphorylation on Akt (Fig. 5.4B). Confirming a potential cross-talk between these two pivotal survival regulators, in which one regulates the other depending on the stress severity and likely also on the site of Akt phosphorylation.

By comparing the two stresses, serum deprivation did not effectively killed cells but rather stopped them slowing their proliferation. Such a difference was also evidenced in Cer species quantification. Considering that Cer is a well-known apoptotic signaling mediator whose cellular content increases upon stress [188] and that its involvement in oxidative stress-induced apoptosis was also documented in photoreceptors [52], we evaluated Cer

content by LC–MS analysis and we observed different profile of Cer.s pools under the two stresses. H_2O_2, which is a direct and immediate ROS mediated damage inducer, causing mitochondria failure and triggering a rapid apoptotic response, induced an augment in long-chain Cer (16:0, 18:0, 20:0 and 22:0), known as pro-apoptotic species [73]. At the same time, it produced a decrease in the very long-chain Cer 24:0. Given that Cer 16:0 and 24:0 are the most abundant species, the total level of Cer resulted unchanged overall. (Fig. 5.6A). SD did not induce any augment in Cer content, on the contrary we observed that all the species were reduced (Fig. 5.6B), according to the necessity to slow down all energy consuming processes, including sphingolipids synthesis.

The evidences that oxidative stress directly influences sphingolipid pathway and, in particular, Cer which is the hub of all the biosynthetic chain, led us to focus our investigation mainly on this kind of stress. Before deepening in biochemical mechanisms, we investigated the influence of THI pretreatment on H_2O_2-stressed photoreceptors, observing that the inhibitor had a significant effect on Cer quantities and succeeded in lowering, not only almost all Cer species analyzed, but also total Cer, because of its indiscriminate action upon different chain-length species (Fig. 5.7).

Furthermore, we investigated S1P amounts modulation under THI and H_2O_2 treatment. Intracellular S1P detection is not easily feasible in comparison with others sphingolipids, given both its low concentration inside the cells and its rapid degradation by means of SPL and phosphatases, although we succeeded in evidencing significant modulation of S1P. In particular, on one side THI treatment promoted S1P raise in photoreceptors (Fig. 5.8A) and on the other side oxidative stress induced its decrease (Fig. 5.8B). Whereas the inhibitor pretreatment on stressed cells did not produce a sufficient effect, indeed S1P increase against

challenged photoreceptors resulted to be not significant, likely due to abovementioned difficulties in its detection (Fig. 5.8C)

Due to the fact that pro-death Cer species increased under oxidative stress and declined in the presence of THI, we investigated apoptosis by TUNEL assay observing, as expected, that the percentage of apoptotic photoreceptors increased after 12 hours of H_2O_2 (Fig. 5.9A). Next, we analyzed and compared the protein expression of two Bcl2 family members with opposed roles: Bcl2, an anti-apoptotic marker, and Bax, a pro-apoptotic one [189]. Apoptosis decrease during retinal development [190] or pharmacological impairment of apoptosis in retina [191] was previously demonstrated to associate with pro-death Bcl-2 proteins content.
Our data, in line with literature, showed a decrease in Bcl2/Bax ratio translating in a predominant relative amount of Bax that could be associated to the apoptosis degree observed with the immunofluorescence test (Fig. 5.9A and B).
By means of FRAP test, a commonly employed method to investigate plasma reducing power [192], we observed that 12 hours of H_2O_2 decreased the amount of reduced iron, that in turn is associated with a diminished release of antioxidant molecules in the colture medium and hence in augmented oxidative stress in cells (Fig. 5.10A).
In order to elucidate the mechanism underlying photoreceptors responses to oxidative stress, we investigated the activation of the nuclear factor erythroid 2 (NFE2)-related factor 2, Nrf2. The latter is a transcription factor with a fundamental role in cell resistance to oxidative stress. In basal condition its activity is suppressed by Keap1 protein (Kelch-like ECH-associated protein 1) through a continuous ubiquitination-proteasomal degradation that is suspended by the action of oxidants and electrophiles, via modification of Keap1 critical cysteine thiols groups and release of Nrf2 [177]. Nrf2 role in 661W cells protection to oxidative stress was previously

observed [193]. Similarly, our data showed a weak however significant increase of Nrf2 expression after H_2O_2 treatment (Fig. 5.10B). When Nrf2 is activated it translocates into the nucleus, where its binding to antioxidant-responsive elements (AREs), stimulates the transcription of phase II genes encoding detoxifying and antioxidant enzymes, such as heme oxygenase-1 (HO-1) [194]. HO-1 protective induction was previously documented in 661W cells [66] [51]. In order to identify a possible involvement of HO-1 activation, in Fig. 5.11, we analyzed its transcript and observed that an increased transcription is associated with early survival response to stress, but after 24 and 48 hours HO-1 mRNA levels fall down in association with cell death progression.

In order to elucidate THI protective mechanism, we investigated the effect of its pretreatment on the above studied signaling mediators. As previously shown, DHA-induced protection of photoreceptors death was attributed to the increased of Bcl2-Bax ratio likely induced by ERK/MAPK activation [195]. Furthermore Bcl2 overexpression was demonstrated to rescue 661W cells from photoxidative stress [24] and to counteract photoreceptors apoptosis in different retinal degenerations [196]. Additionally, in Jurkat cells, S1P inhibition of the pro-apoptotic Bax and Bad activation, was supposed to be caused by MEK activation [197].

In our hands, THI pretreatment was able to reduce apoptosis, decreasing the number of TUNEL-stained cells with respect to only stressed cells (Fig. 5.12A). Simultaneously Bcl2 expression augmented up to overtake that of Bax, shifting their ratio equilibrium in favour to survival stimulus and proving that the inhibition of S1P degradation has a role in preserving 661W cells from apoptosis (Fig. 5.12B). Moreover, THI showed an antioxidant activity against H_2O_2, augmenting the FRAP value (Fig. 5.13A) and further stabilizing Nrf2 protein in stressed cells (Fig. 5.13B), thus supporting the hypothesis of a critical role of the transcription factor in cells protection. In THI and H_2O_2 treated cells, HO-1 transcription was protracted, in

accordance with Nrf2 stabilization. Whereas after 48 hours of H_2O_2 HO-1 transcription was repressed, in THI pretreated cells the transcript is still present at high levels, likely as a part of the THI induced survival response, the higher difference was at 48 hours (Fig. 5.14). We can conclude that one of the downstream effect of THI is to strengthen the action of detoxification enzymes. This may be imputable to an indirect S1P antioxidant induction against oxidative stress, resulting in an enriched response of detoxifying pathways. Similarly, in a rat model of emphysema, S1P ability to overexpress Nrf2 against stress was previously showed [198], in addition Nrf2 was showed to protect human RPE cells from H_2O_2-induced oxidative stress via Nrf2-mediated upregulation of the expression of phase II enzymes involving the PI3K/Akt pathway [199]. Furthermore HO-1 induction protected retinal ganglion cells in diabetic retinopathy [200], even if it was also demonstrated that decreased expression of HO-1 was observed in treatments with molecules that acted as direct scavengers against H_2O_2 [201].

Given S1P duality as intracellular messenger and extracellular ligand and its well-know ability to exit the cell through specific transporters [202], we hypothesized that THI, by means of S1P accumulation, could interact or modulate S1PRs. To the best of our knowledge, the expression of S1PRs has not been proven in 661W cell line. Analyzing S1P1-5 mRNA we confirmed their expression in our cellular model and underlined different and proportional decreasing degree of receptor's expression. In particular, S1P1 resulted to be the more abundant member, followed by S1P2, whereas S1P3-5 showed the lowest expression (Fig. 5.15). S1PRs belong to the family of GPCR proteins, they are coupled to different G-proteins and, for this reason, their influence on cells behaviour widely changes [110].

Preliminary data on THI effect on S1PRs expression showed an interesting tendency in a preferential modulation of S1P4 and S1P5. THI alone increased both mRNA receptors and did not significantly alter S1P1-3, especially for what concerned the second receptor (Fig. 5.16). In contrast, oxidative stress had a negative influence on transcript amounts, powerfully acting on S1P3-5, as emerged from Fig. 5.17. THI pretreatment on stressed photoreceptors strongly overexpressed S1P4 and S1P5 and showed a weak however significant activity also on S1P1 (Fig. 5.18). In conclusion S1P2 resulted to be the only member of S1PRs family, in 661W, that was affected neither by THI nor by oxidative stress effects. All these observations, although they must be further confirmed, have to be considered interesting and significant in the global vision for putative THI purpose in visual and, in particular, neural-retinal pathologies, opening the possibility of new therapeutic strategies. Therefore, we distinguished a double THI effect in antagonizing oxidative stress: firstly, its action on cell proliferation, viability, apoptosis and oxidant power and, secondly, its ability to modulate S1PRs expression in unstressed and stressed photoreceptors.

Given the interesting modulation of S1PRs in our *in vitro* model, we investigated the involvement of exogenous S1P in 661W cells rescue from oxidative stress. Cells were pretreated for 1 hour with S1P at 1μM and then challenged with H_2O_2 1mM for 12, 24 and 48 hours. Exogenously added S1P did not show significant cellular proliferation improvement against oxidative stress (Fig. 5.19A). Being GPCR, S1PRs underwent desensitization via temporary or β-arrestin-induced internalization upon massive engagement by respectively S1P or its potent agonists [111]. As a matter of fact, lowering exogenous S1P concentration to 100nM, we obtained a remarkable rescue from cellular proliferation arrest upon oxidative stress (Fig. 5.19B). We confirmed that low S1P concentration increased cell viability after 12 hours of oxidative stress, (Fig. 5.19C). In line

with previous investigations, we measured FRAP value after S1P treatment obtaining an augment in antioxidant induced power respect to stressed cells (Fig. 5.20).

To strengthen our hypothesis on the pivotal role of sphingolipids in photoreceptors fate and on the importance of their biosynthetic pathway manipulation, as a tool in contrasting retinal degeneration, we focused on Cer modulation employing a potent inhibitor of its *de novo* synthesis, Myriocin. This inhibitor was, previously, employed *in vivo* by our group demonstrating that inhibition of Cer *de novo* synthesis is able to rescue photoreceptors from degeneration, in a RP murine model [143]. We hypothesized that inhibition of Cer generation and increase of S1P intracellular content may be combined in the intent of improving cell protection. At this aim cells were treated with Myriocin (10 µM) also in the presence of THI (75 µM) for 5 hours and then H_2O_2 (1mM) was added for other 12 hours. LC-MS analysis confirmed that Myriocin drastically reduced all Cer species (Fig. 5.22), suggesting that *de novo* synthesis of Cer is majorly involved in oxidative stress in 661W. Unexpectedly, the combination of the two inhibitors failed to allow additive protection from cell death (Fig. 5.23); moreover it did not increase the production of antioxidant molecules (Fig. 5.24) under H_2O_2 treatment. This data lead to hypothesize that S1P protection and Cer induced apoptosis signal through pathways that are somehow interconnected, as indicated by THI modulation of some Cer species.

THI is supposed to interact with PLP, the SPL cofactor, blocking its normal involvement in enzymatic mechanism to degrade S1P [149]. This hypothesis is supported by the evidence of vitamin B6 opposition to THI effect [154]. In our case, due to the pivotal role of PLP in SPT activity, this should be an explanation for decreased Cer amounts that we observed in

THI pretreated cells, even if significant modulation was registered only after oxidative stimulus (Fig. 5.21). This last observation together with the recent hypothesis defining SphK-1 and SphK-2 as regulators of *de novo* Cer synthesis [99], suggest the existence of a feedback action of S1P on Cer synthesis as previously demonstrated for phosphorylated long-chain sphingoid bases [203]. Oxidative stress induced apoptotic Cer generation. However, in THI pretreated cells, accumulated S1P modulates Cer, triggering their decrease. Both hypothesis look to the *de novo* pathway rather than to the salvage one, especially if we consider THI similitude to Myriocin in the indiscriminately way to induce Cer amount modulations.

The pivotal role of Myriocin SPT inhibition in physiological and pathological states was demonstrated. Given the high cost of this inhibitor, we screened 30 new synthesized compounds as putative SPT inhibitors. We were able to evidenced three molecules that led to a residue SPT activity equal to, at least, 30%. The IC50 of these new inhibitors was calculated (Tab. 1). Even if Myriocin effect remains incomparable, the identification of putative new structures leaves the way open to further investigations. An important association is underlined between some functional groups and the increase of SPT activity. To date, this trend is noticed in 4 compounds (A7, DC6, DC11 and DC12). This analysis is still ongoing in our laboratories.

7. CONCLUSIONS

In conclusion S1P endogenous increase, obtained with THI treatment, favours survival and proliferation upon stresses in an *in vitro* model of photoreceptor degeneration. S1P effect, against oxidative stress, is linked to some crucial intracellular pathways involved in cell fate regulation. Indeed, it modulates ERK and Akt activation, Bcl-2/Bax equilibrium, Nrf2-HO-1 expression and reduced intracellular Cer amounts (Fig. 7.1).

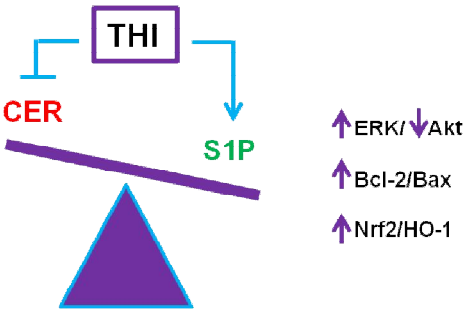

Fig. 7.1: Conclusion scheme. THI accumulation of S1P induces decrease of apoptotic Cer and activates intracellular survival pathways.

From our preliminary data, we can also conclude that THI-induced increase of S1P influences S1PRs expression. In addition, to confirm a supplementary role of extracellular S1P, we show that low exogenous S1P counteracts the inhibition of photoreceptors proliferation and viability induced by oxidative stress. Moreover, the cotreatment with inhibitors of sphingolipid synthesis and degradation, reducing Cer and increasing S1P intracellular content, is able to ensure survival in response to oxidative stress, even if the hypothesized addictive effect was not observed.

All these outcomes together demonstrate and confirm sphingolipid biosynthetic pathway as a paramount target in therapeutic approaches for photoreceptor degeneration.

8. REFERENCES

1. Strauss, O., *The retinal pigment epithelium in visual function.* Physiol Rev, 2005. **85**(3): p. 845-81.
2. Purves D., A.G., Fitzpatrick D et al., *Neuroscience. 2nd edition*. 2001, Sunderland (MA): Sinauer Associates.
3. Kefalov, V.J., *Rod and cone visual pigments and phototransduction through pharmacological, genetic, and physiological approaches.* J Biol Chem, 2012. **287**(3): p. 1635-41.
4. Kolbe H, F.E., Nelson R, editors, *Webvision: The organization of the Retina and the visual system*. 1995, Salt Lake City (UT): University of Utah Health Sciences Center.
5. Yau, K.W. and R.C. Hardie, *Phototransduction motifs and variations.* Cell, 2009. **139**(2): p. 246-64.
6. Tang, P.H., et al., *New insights into retinoid metabolism and cycling within the retina.* Prog Retin Eye Res, 2013. **32**: p. 48-63.
7. Athanasiou, D., et al., *The cell stress machinery and retinal degeneration.* FEBS Lett, 2013. **587**(13): p. 2008-17.
8. Hartong, D.T., E.L. Berson, and T.P. Dryja, *Retinitis pigmentosa.* Lancet, 2006. **368**(9549): p. 1795-809.
9. Ferrari, S., et al., *Retinitis pigmentosa: genes and disease mechanisms.* Curr Genomics, 2011. **12**(4): p. 238-49.
10. Kajiwara, K., E.L. Berson, and T.P. Dryja, *Digenic retinitis pigmentosa due to mutations at the unlinked peripherin/RDS and ROM1 loci.* Science, 1994. **264**(5165): p. 1604-8.
11. Bhattacharya, S.S., et al., *Close genetic linkage between X-linked retinitis pigmentosa and a restriction fragment length polymorphism identified by recombinant DNA probe L1.28.* Nature, 1984. **309**(5965): p. 253-5.
12. Goldberg, A.F., C.J. Loewen, and R.S. Molday, *Cysteine residues of photoreceptor peripherin/rds: role in subunit assembly and autosomal dominant retinitis pigmentosa.* Biochemistry, 1998. **37**(2): p. 680-5.
13. Travis, G.H., et al., *Identification of a photoreceptor-specific mRNA encoded by the gene responsible for retinal degeneration slow (rds).* Nature, 1989. **338**(6210): p. 70-3.
14. van Soest, S., et al., *Retinitis pigmentosa: defined from a molecular point of view.* Surv Ophthalmol, 1999. **43**(4): p. 321-34.
15. Dryja, T.P., et al., *A point mutation of the rhodopsin gene in one form of retinitis pigmentosa.* Nature, 1990. **343**(6256): p. 364-6.
16. Dryja, T.P. and T. Li, *Molecular genetics of retinitis pigmentosa.* Hum Mol Genet, 1995. **4 Spec No**: p. 1739-43.
17. Tuson, M., G. Marfany, and R. Gonzalez-Duarte, *Mutation of CERKL, a novel human ceramide kinase gene, causes autosomal recessive retinitis pigmentosa (RP26).* Am J Hum Genet, 2004. **74**(1): p. 128-38.
18. Wright, A.F., et al., *Photoreceptor degeneration: genetic and mechanistic dissection of a complex trait.* Nat Rev Genet, 2010. **11**(4): p. 273-84.
19. Portera-Cailliau, C., et al., *Apoptotic photoreceptor cell death in mouse models of retinitis pigmentosa.* Proc Natl Acad Sci U S A, 1994. **91**(3): p. 974-8.
20. Wenzel, A., et al., *Molecular mechanisms of light-induced photoreceptor apoptosis and neuroprotection for retinal degeneration.* Prog Retin Eye Res, 2005. **24**(2): p. 275-306.

21. Sancho-Pelluz, J., et al., *Photoreceptor cell death mechanisms in inherited retinal degeneration.* Mol Neurobiol, 2008. **38**(3): p. 253-69.
22. Gomez-Vicente, V., M. Donovan, and T.G. Cotter, *Multiple death pathways in retina-derived 661W cells following growth factor deprivation: crosstalk between caspases and calpains.* Cell Death Differ, 2005. **12**(7): p. 796-804.
23. Nir, I., et al., *Expression of Bcl-2 protects against photoreceptor degeneration in retinal degeneration slow (rds) mice.* J Neurosci, 2000. **20**(6): p. 2150-4.
24. Crawford, M.J., et al., *Bcl-2 overexpression protects photooxidative stress-induced apoptosis of photoreceptor cells via NF-kappaB preservation.* Biochem Biophys Res Commun, 2001. **281**(5): p. 1304-12.
25. Quiambao, A.B., et al., *Transgenic Bcl-2 expressed in photoreceptor cells confers both death-sparing and death-inducing effects.* Exp Eye Res, 2001. **73**(5): p. 711-21.
26. Cottet, S. and D.F. Schorderet, *Mechanisms of apoptosis in retinitis pigmentosa.* Curr Mol Med, 2009. **9**(3): p. 375-83.
27. Zacks, D.N., et al., *FAS-mediated apoptosis and its relation to intrinsic pathway activation in an experimental model of retinal detachment.* Invest Ophthalmol Vis Sci, 2004. **45**(12): p. 4563-9.
28. Murakami, Y., et al., *Photoreceptor cell death and rescue in retinal detachment and degenerations.* Prog Retin Eye Res, 2013. **37**: p. 114-40.
29. Kunchithapautham, K. and B. Rohrer, *Apoptosis and autophagy in photoreceptors exposed to oxidative stress.* Autophagy, 2007. **3**(5): p. 433-41.
30. Rotstein, N.P., et al., *Regulating survival and development in the retina: key roles for simple sphingolipids.* J Lipid Res, 2010. **51**(6): p. 1247-62.
31. Trifunovic, D., et al., *Neuroprotective strategies for the treatment of inherited photoreceptor degeneration.* Curr Mol Med, 2012. **12**(5): p. 598-612.
32. Petrs-Silva, H. and R. Linden, *Advances in gene therapy technologies to treat retinitis pigmentosa.* Clin Ophthalmol, 2014. **8**: p. 127-136.
33. Seiler, M.J. and R.B. Aramant, *Cell replacement and visual restoration by retinal sheet transplants.* Prog Retin Eye Res, 2012. **31**(6): p. 661-87.
34. Chuang, A.T., C.E. Margo, and P.B. Greenberg, *Retinal implants: a systematic review.* Br J Ophthalmol, 2014.
35. Stingl, K., et al., *Artificial vision with wirelessly powered subretinal electronic implant alpha-IMS.* Proc Biol Sci, 2013. **280**(1757): p. 20130077.
36. Garg, S.J. and J. Federman, *Optogenetics, visual prosthesis and electrostimulation for retinal dystrophies.* Curr Opin Ophthalmol, 2013. **24**(5): p. 407-14.
37. Bi, A., et al., *Ectopic expression of a microbial-type rhodopsin restores visual responses in mice with photoreceptor degeneration.* Neuron, 2006. **50**(1): p. 23-33.
38. Schatz, A., et al., *Transcorneal electrical stimulation for patients with retinitis pigmentosa: a prospective, randomized, sham-controlled exploratory study.* Invest Ophthalmol Vis Sci, 2011. **52**(7): p. 4485-96.

39. Kolomeyer, A.M. and M.A. Zarbin, *Trophic factors in the pathogenesis and therapy for retinal degenerative diseases.* Surv Ophthalmol, 2014. **59**(2): p. 134-65.
40. Perusek, L. and T. Maeda, *Vitamin A derivatives as treatment options for retinal degenerative diseases.* Nutrients, 2013. **5**(7): p. 2646-66.
41. Hoffman, D.R., et al., *Four-Year Placebo-Controlled Trial of Docosahexaenoic Acid in X-Linked Retinitis Pigmentosa (DHAX Trial): A Randomized Clinical Trial.* JAMA Ophthalmol, 2014.
42. Berson, E.L., et al., *Clinical trial of lutein in patients with retinitis pigmentosa receiving vitamin A.* Arch Ophthalmol, 2010. **128**(4): p. 403-11.
43. Froger, N., et al., *Taurine: The comeback of a neutraceutical in the prevention of retinal degenerations.* Prog Retin Eye Res, 2014.
44. Dunn, K.C., et al., *ARPE-19, a human retinal pigment epithelial cell line with differentiated properties.* Exp Eye Res, 1996. **62**(2): p. 155-69.
45. Krishnamoorthy, R.R., et al., *Characterization of a transformed rat retinal ganglion cell line.* Brain Res Mol Brain Res, 2001. **86**(1-2): p. 1-12.
46. Seigel, G.M., *Review: R28 retinal precursor cells: The first 20 years.* Mol Vis, 2014. **20**: p. 301-306.
47. al-Ubaidi, M.R., et al., *Bilateral retinal and brain tumors in transgenic mice expressing simian virus 40 large T antigen under control of the human interphotoreceptor retinoid-binding protein promoter.* J Cell Biol, 1992. **119**(6): p. 1681-7.
48. Tan, E., et al., *Expression of cone-photoreceptor-specific antigens in a cell line derived from retinal tumors in transgenic mice.* Invest Ophthalmol Vis Sci, 2004. **45**(3): p. 764-8.
49. Kanan, Y., et al., *Light induces programmed cell death by activating multiple independent proteases in a cone photoreceptor cell line.* Invest Ophthalmol Vis Sci, 2007. **48**(1): p. 40-51.
50. Tanaka, J., et al., *Purple rice extract and anthocyanidins of the constituents protect against light-induced retinal damage in vitro and in vivo.* J Agric Food Chem, 2011. **59**(2): p. 528-36.
51. Chen, H., et al., *Caffeic acid phenethyl ester protects 661W cells from H2O2-mediated cell death and enhances electroretinography response in dim-reared albino rats.* Mol Vis, 2012. **18**: p. 1325-38.
52. Sanvicens, N., et al., *Oxidative stress-induced apoptosis in retinal photoreceptor cells is mediated by calpains and caspases and blocked by the oxygen radical scavenger CR-6.* J Biol Chem, 2004. **279**(38): p. 39268-78.
53. Wang, J., et al., *Direct effect of sodium iodate on neurosensory retina.* Invest Ophthalmol Vis Sci, 2014.
54. Abrahan, C.E., et al., *Synthesis of sphingosine is essential for oxidative stress-induced apoptosis of photoreceptors.* Invest Ophthalmol Vis Sci, 2010. **51**(2): p. 1171-80.
55. Roque, R.S., et al., *Retina-derived microglial cells induce photoreceptor cell death in vitro.* Brain Res, 1999. **836**(1-2): p. 110-9.
56. Sheedlo, H.J., et al., *RPE-derived factors modulate photoreceptor differentiation: a possible role in the retinal stem cell niche.* In Vitro Cell Dev Biol Anim, 2007. **43**(10): p. 361-70.

57. Rapp, M., et al., *Pigment Epithelium-Derived Factor Protects Cone Photoreceptor-Derived 661W Cells from Light Damage Through Akt Activation.* Adv Exp Med Biol, 2014. **801**: p. 813-20.
58. Yang, L.P., X.A. Zhu, and M.O. Tso, *A possible mechanism of microglia-photoreceptor crosstalk.* Mol Vis, 2007. **13**: p. 2048-57.
59. Wassmer, S., et al., *Chitosan microparticles for delivery of proteins to the retina.* Acta Biomater, 2013. **9**(8): p. 7855-64.
60. Schnichels, S., et al., *Comparative toxicity and proliferation testing of aflibercept, bevacizumab and ranibizumab on different ocular cells.* Br J Ophthalmol, 2013. **97**(7): p. 917-23.
61. Zhou, W.T., et al., *Electrical stimulation ameliorates light-induced photoreceptor degeneration in vitro via suppressing the proinflammatory effect of microglia and enhancing the neurotrophic potential of Muller cells.* Exp Neurol, 2012. **238**(2): p. 192-208.
62. Fliesler, S.J. and R.E. Anderson, *Chemistry and metabolism of lipids in the vertebrate retina.* Prog Lipid Res, 1983. **22**(2): p. 79-131.
63. Sharma, A.K. and B. Rohrer, *Sustained elevation of intracellular cGMP causes oxidative stress triggering calpain-mediated apoptosis in photoreceptor degeneration.* Curr Eye Res, 2007. **32**(3): p. 259-69.
64. Tsuruma, K., et al., *Unoprostone reduces oxidative stress- and light-induced retinal cell death, and phagocytotic dysfunction, by activating BK channels.* Mol Vis, 2011. **17**: p. 3556-65.
65. Rezaie, T., et al., *Protective effect of carnosic acid, a pro-electrophilic compound, in models of oxidative stress and light-induced retinal degeneration.* Invest Ophthalmol Vis Sci, 2012. **53**(12): p. 7847-54.
66. Mandal, M.N., et al., *Curcumin protects retinal cells from light-and oxidant stress-induced cell death.* Free Radic Biol Med, 2009. **46**(5): p. 672-9.
67. Wheeler, T.G., R.M. Benolken, and R.E. Anderson, *Visual membranes: specificity of fatty acid precursors for the electrical response to illumination.* Science, 1975. **188**(4195): p. 1312-4.
68. Hannun, Y.A. and L.M. Obeid, *Principles of bioactive lipid signalling: lessons from sphingolipids.* Nat Rev Mol Cell Biol, 2008. **9**(2): p. 139-50.
69. Gault, C.R., L.M. Obeid, and Y.A. Hannun, *An overview of sphingolipid metabolism: from synthesis to breakdown.* Adv Exp Med Biol, 2010. **688**: p. 1-23.
70. Kitatani, K., J. Idkowiak-Baldys, and Y.A. Hannun, *The sphingolipid salvage pathway in ceramide metabolism and signaling.* Cell Signal, 2008. **20**(6): p. 1010-8.
71. Mitra, P., et al., *Role of ABCC1 in export of sphingosine-1-phosphate from mast cells.* Proc Natl Acad Sci U S A, 2006. **103**(44): p. 16394-9.
72. Boujaoude, L.C., et al., *Cystic fibrosis transmembrane regulator regulates uptake of sphingoid base phosphates and lysophosphatidic acid: modulation of cellular activity of sphingosine 1-phosphate.* J Biol Chem, 2001. **276**(38): p. 35258-64.
73. Grosch, S., S. Schiffmann, and G. Geisslinger, *Chain length-specific properties of ceramides.* Prog Lipid Res, 2012. **51**(1): p. 50-62.
74. Hannun, Y.A. and L.M. Obeid, *Many ceramides.* J Biol Chem, 2011. **286**(32): p. 27855-62.

75. Hannun, Y.A. and L.M. Obeid, *The Ceramide-centric universe of lipid-mediated cell regulation: stress encounters of the lipid kind.* J Biol Chem, 2002. **277**(29): p. 25847-50.
76. Chalfant, C.E., et al., *Long chain ceramides activate protein phosphatase-1 and protein phosphatase-2A. Activation is stereospecific and regulated by phosphatidic acid.* J Biol Chem, 1999. **274**(29): p. 20313-7.
77. Ruvolo, P.P., et al., *Ceramide induces Bcl2 dephosphorylation via a mechanism involving mitochondrial PP2A.* J Biol Chem, 1999. **274**(29): p. 20296-300.
78. Xin, M. and X. Deng, *Protein phosphatase 2A enhances the proapoptotic function of Bax through dephosphorylation.* J Biol Chem, 2006. **281**(27): p. 18859-67.
79. Heinrich, M., et al., *Ceramide as an activator lipid of cathepsin D.* Adv Exp Med Biol, 2000. **477**: p. 305-15.
80. Xing, H.R., J. Lozano, and R. Kolesnick, *Epidermal growth factor treatment enhances the kinase activity of kinase suppressor of Ras.* J Biol Chem, 2000. **275**(23): p. 17276-80.
81. Lozano, J., et al., *Protein kinase C zeta isoform is critical for kappa B-dependent promoter activation by sphingomyelinase.* J Biol Chem, 1994. **269**(30): p. 19200-2.
82. Zhang, H., et al., *Sphingosine-1-phosphate, a novel lipid, involved in cellular proliferation.* J Cell Biol, 1991. **114**(1): p. 155-67.
83. Maceyka, M., et al., *Sphingosine-1-phosphate signaling and its role in disease.* Trends Cell Biol, 2012. **22**(1): p. 50-60.
84. Mendelson, K., T. Evans, and T. Hla, *Sphingosine 1-phosphate signalling.* Development, 2014. **141**(1): p. 5-9.
85. Kupperman, E., et al., *A sphingosine-1-phosphate receptor regulates cell migration during vertebrate heart development.* Nature, 2000. **406**(6792): p. 192-5.
86. Chae, S.S., et al., *Regulation of limb development by the sphingosine 1-phosphate receptor S1p1/EDG-1 occurs via the hypoxia/VEGF axis.* Dev Biol, 2004. **268**(2): p. 441-7.
87. Mizugishi, K., et al., *Essential role for sphingosine kinases in neural and vascular development.* Mol Cell Biol, 2005. **25**(24): p. 11113-21.
88. Gaengel, K., et al., *The sphingosine-1-phosphate receptor S1PR1 restricts sprouting angiogenesis by regulating the interplay between VE-cadherin and VEGFR2.* Dev Cell, 2012. **23**(3): p. 587-99.
89. Takabe, K., et al., *"Inside-out" signaling of sphingosine-1-phosphate: therapeutic targets.* Pharmacol Rev, 2008. **60**(2): p. 181-95.
90. Young, K.W. and S.R. Nahorski, *Intracellular sphingosine 1-phosphate production: a novel pathway for Ca2+ release.* Semin Cell Dev Biol, 2001. **12**(1): p. 19-25.
91. Maceyka, M., et al., *Sphingosine kinase, sphingosine-1-phosphate, and apoptosis.* Biochim Biophys Acta, 2002. **1585**(2-3): p. 193-201.
92. Xia, P., et al., *Tumor necrosis factor-alpha induces adhesion molecule expression through the sphingosine kinase pathway.* Proc Natl Acad Sci U S A, 1998. **95**(24): p. 14196-201.

93. Osawa, Y., et al., *TNF-alpha-induced sphingosine 1-phosphate inhibits apoptosis through a phosphatidylinositol 3-kinase/Akt pathway in human hepatocytes.* J Immunol, 2001. **167**(1): p. 173-80.
94. Shatrov, V.A., V. Lehmann, and S. Chouaib, *Sphingosine-1-phosphate mobilizes intracellular calcium and activates transcription factor NF-kappa B in U937 cells.* Biochem Biophys Res Commun, 1997. **234**(1): p. 121-4.
95. Goetzl, E.J., Y. Kong, and B. Mei, *Lysophosphatidic acid and sphingosine 1-phosphate protection of T cells from apoptosis in association with suppression of Bax.* J Immunol, 1999. **162**(4): p. 2049-56.
96. An, S., Y. Zheng, and T. Bleu, *Sphingosine 1-phosphate-induced cell proliferation, survival, and related signaling events mediated by G protein-coupled receptors Edg3 and Edg5.* J Biol Chem, 2000. **275**(1): p. 288-96.
97. Kwon, Y.G., et al., *Sphingosine 1-phosphate protects human umbilical vein endothelial cells from serum-deprived apoptosis by nitric oxide production.* J Biol Chem, 2001. **276**(14): p. 10627-33.
98. Lee, M.J., et al., *Vascular endothelial cell adherens junction assembly and morphogenesis induced by sphingosine-1-phosphate.* Cell, 1999. **99**(3): p. 301-12.
99. Maceyka, M., et al., *SphK1 and SphK2, sphingosine kinase isoenzymes with opposing functions in sphingolipid metabolism.* J Biol Chem, 2005. **280**(44): p. 37118-29.
100. Orr Gandy, K.A. and L.M. Obeid, *Targeting the sphingosine kinase/sphingosine 1-phosphate pathway in disease: review of sphingosine kinase inhibitors.* Biochim Biophys Acta, 2013. **1831**(1): p. 157-66.
101. Olivera, A., et al., *Sphingosine kinase expression increases intracellular sphingosine-1-phosphate and promotes cell growth and survival.* J Cell Biol, 1999. **147**(3): p. 545-58.
102. Pitson, S.M., et al., *Activation of sphingosine kinase 1 by ERK1/2-mediated phosphorylation.* EMBO J, 2003. **22**(20): p. 5491-500.
103. Hait, N.C., et al., *Sphingosine kinase type 2 activation by ERK-mediated phosphorylation.* J Biol Chem, 2007. **282**(16): p. 12058-65.
104. Neubauer, H.A. and S.M. Pitson, *Roles, regulation and inhibitors of sphingosine kinase 2.* FEBS J, 2013. **280**(21): p. 5317-36.
105. Liu, H., et al., *Sphingosine kinase type 2 is a putative BH3-only protein that induces apoptosis.* J Biol Chem, 2003. **278**(41): p. 40330-6.
106. Chumanevich, A.A., et al., *Suppression of colitis-driven colon cancer in mice by a novel small molecule inhibitor of sphingosine kinase.* Carcinogenesis, 2010. **31**(10): p. 1787-93.
107. Vessey, D.A., et al., *A sphingosine kinase form 2 knockout sensitizes mouse myocardium to ischemia/reoxygenation injury and diminishes responsiveness to ischemic preconditioning.* Oxid Med Cell Longev, 2011. **2011**: p. 961059.
108. Goodemote, K.A., et al., *Involvement of a pertussis toxin-sensitive G protein in the mitogenic signaling pathways of sphingosine 1-phosphate.* J Biol Chem, 1995. **270**(17): p. 10272-7.
109. Lee, M.J., et al., *Sphingosine-1-phosphate as a ligand for the G protein-coupled receptor EDG-1.* Science, 1998. **279**(5356): p. 1552-5.

110. Brinkmann, V., *Sphingosine 1-phosphate receptors in health and disease: mechanistic insights from gene deletion studies and reverse pharmacology.* Pharmacol Ther, 2007. **115**(1): p. 84-105.
111. Rosen, H., et al., *Sphingosine 1-phosphate receptor signaling.* Annu Rev Biochem, 2009. **78**: p. 743-68.
112. Matloubian, M., et al., *Lymphocyte egress from thymus and peripheral lymphoid organs is dependent on S1P receptor 1.* Nature, 2004. **427**(6972): p. 355-60.
113. Kitano, M., et al., *Sphingosine 1-phosphate/sphingosine 1-phosphate receptor 1 signaling in rheumatoid synovium: regulation of synovial proliferation and inflammatory gene expression.* Arthritis Rheum, 2006. **54**(3): p. 742-53.
114. Li, M.H., et al., *S1P/S1P1 signaling stimulates cell migration and invasion in Wilms tumor.* Cancer Lett, 2009. **276**(2): p. 171-9.
115. Sanchez, T., et al., *Induction of vascular permeability by the sphingosine-1-phosphate receptor-2 (S1P2R) and its downstream effectors ROCK and PTEN.* Arterioscler Thromb Vasc Biol, 2007. **27**(6): p. 1312-8.
116. Skoura, A., et al., *Essential role of sphingosine 1-phosphate receptor 2 in pathological angiogenesis of the mouse retina.* J Clin Invest, 2007. **117**(9): p. 2506-16.
117. Adada, M., et al., *Sphingosine-1-phosphate receptor 2.* FEBS J, 2013. **280**(24): p. 6354-66.
118. Bajwa, A., et al., *Dendritic cell sphingosine 1-phosphate receptor-3 regulates Th1-Th2 polarity in kidney ischemia-reperfusion injury.* J Immunol, 2012. **189**(5): p. 2584-96.
119. Van Doorn, R., et al., *Sphingosine 1-phosphate receptor 1 and 3 are upregulated in multiple sclerosis lesions.* Glia, 2010. **58**(12): p. 1465-76.
120. Fischer, I., et al., *Sphingosine kinase 1 and sphingosine 1-phosphate receptor 3 are functionally upregulated on astrocytes under pro-inflammatory conditions.* PLoS One, 2011. **6**(8): p. e23905.
121. Schulze, T., et al., *Sphingosine-1-phospate receptor 4 (S1P(4)) deficiency profoundly affects dendritic cell function and TH17-cell differentiation in a murine model.* FASEB J, 2011. **25**(11): p. 4024-36.
122. Jaillard, C., et al., *Edg8/S1P5: an oligodendroglial receptor with dual function on process retraction and cell survival.* J Neurosci, 2005. **25**(6): p. 1459-69.
123. van Doorn, R., et al., *Sphingosine 1-phosphate receptor 5 mediates the immune quiescence of the human brain endothelial barrier.* J Neuroinflammation, 2012. **9**: p. 133.
124. Hu, W.M., et al., *Effect of S1P5 on proliferation and migration of human esophageal cancer cells.* World J Gastroenterol, 2010. **16**(15): p. 1859-66.
125. Bourquin, F., G. Capitani, and M.G. Grutter, *PLP-dependent enzymes as entry and exit gates of sphingolipid metabolism.* Protein Sci, 2011. **20**(9): p. 1492-508.
126. Hornemann, T., et al., *Cloning and initial characterization of a new subunit for mammalian serine-palmitoyltransferase.* J Biol Chem, 2006. **281**(49): p. 37275-81.
127. Lowther, J., et al., *Structural, mechanistic and regulatory studies of serine palmitoyltransferase.* Biochem Soc Trans, 2012. **40**(3): p. 547-54.

128. Linn, S.C., et al., *Regulation of de novo sphingolipid biosynthesis and the toxic consequences of its disruption.* Biochem Soc Trans, 2001. **29**(Pt 6): p. 831-5.
129. Memon, R.A., et al., *Endotoxin and cytokines increase hepatic sphingolipid biosynthesis and produce lipoproteins enriched in ceramides and sphingomyelin.* Arterioscler Thromb Vasc Biol, 1998. **18**(8): p. 1257-65.
130. Farrell, A.M., et al., *UVB irradiation up-regulates serine palmitoyltransferase in cultured human keratinocytes.* J Lipid Res, 1998. **39**(10): p. 2031-8.
131. Fyrst, H. and J.D. Saba, *Sphingosine-1-phosphate lyase in development and disease: sphingolipid metabolism takes flight.* Biochim Biophys Acta, 2008. **1781**(9): p. 448-58.
132. Aguilar, A. and J.D. Saba, *Truth and consequences of sphingosine-1-phosphate lyase.* Adv Biol Regul, 2012. **52**(1): p. 17-30.
133. Oskouian, B., et al., *Sphingosine-1-phosphate lyase potentiates apoptosis via p53- and p38-dependent pathways and is down-regulated in colon cancer.* Proc Natl Acad Sci U S A, 2006. **103**(46): p. 17384-9.
134. Ramaswamy, S., et al., *A molecular signature of metastasis in primary solid tumors.* Nat Genet, 2003. **33**(1): p. 49-54.
135. Paris, F., et al., *Sphingosine 1-phosphate preserves fertility in irradiated female mice without propagating genomic damage in offspring.* Nat Med, 2002. **8**(9): p. 901-2.
136. Kluepfel, D., et al., *Myriocin, a new antifungal antibiotic from Myriococcum albomyces.* J Antibiot (Tokyo), 1972. **25**(2): p. 109-15.
137. Aragozzini, F., et al., *Structure of thermozymocidin.* Experientia, 1972. **28**(8): p. 881-2.
138. Fujita, T., et al., *Fungal metabolites. Part 11. A potent immunosuppressive activity found in Isaria sinclairii metabolite.* J Antibiot (Tokyo), 1994. **47**(2): p. 208-15.
139. Miyake, Y., et al., *Serine palmitoyltransferase is the primary target of a sphingosine-like immunosuppressant, ISP-1/myriocin.* Biochem Biophys Res Commun, 1995. **211**(2): p. 396-403.
140. Jiang, Q., et al., *gamma-Tocopherol or combinations of vitamin E forms induce cell death in human prostate cancer cells by interrupting sphingolipid synthesis.* Proc Natl Acad Sci U S A, 2004. **101**(51): p. 17825-30.
141. Choi, K.E., et al., *Myriocin induces apoptotic lung cancer cell death via activation of DR4 pathway.* Arch Pharm Res, 2014. **37**(4): p. 501-11.
142. Lee, Y.S., et al., *Myriocin, a serine palmitoyltransferase inhibitor, suppresses tumor growth in a murine melanoma model by inhibiting de novo sphingolipid synthesis.* Cancer Biol Ther, 2012. **13**(2): p. 92-100.
143. Strettoi, E., et al., *Inhibition of ceramide biosynthesis preserves photoreceptor structure and function in a mouse model of retinitis pigmentosa.* Proc Natl Acad Sci U S A, 2010. **107**(43): p. 18706-11.
144. Podbielska, M., H. Krotkiewski, and E.L. Hogan, *Signaling and regulatory functions of bioactive sphingolipids as therapeutic targets in multiple sclerosis.* Neurochem Res, 2012. **37**(6): p. 1154-69.

145. Yang, G., et al., *Central role of ceramide biosynthesis in body weight regulation, energy metabolism, and the metabolic syndrome.* Am J Physiol Endocrinol Metab, 2009. **297**(1): p. E211-24.
146. Jiang, X.C., I.J. Goldberg, and T.S. Park, *Sphingolipids and cardiovascular diseases: lipoprotein metabolism, atherosclerosis and cardiomyopathy.* Adv Exp Med Biol, 2011. **721**: p. 19-39.
147. Wadsworth, J.M., et al., *The chemical basis of serine palmitoyltransferase inhibition by myriocin.* J Am Chem Soc, 2013. **135**(38): p. 14276-85.
148. Billich, A., et al., *Cellular assay for the characterization of sphingosine-1-phosphate lyase inhibitors.* Anal Biochem, 2013. **434**(2): p. 247-53.
149. Bigaud, M., et al., *Second generation S1P pathway modulators: research strategies and clinical developments.* Biochim Biophys Acta, 2014. **1841**(5): p. 745-58.
150. Bagdanoff, J.T., et al., *Inhibition of sphingosine-1-phosphate lyase for the treatment of autoimmune disorders.* J Med Chem, 2009. **52**(13): p. 3941-53.
151. Sinkeldam, E.J., et al., *The effect of pyridoxine on the number of lymphocytes in the blood of rats fed caramel colour (III).* Food Chem Toxicol, 1988. **26**(3): p. 195-203.
152. Iscaro, A., I.R. Mackay, and C. O'Brien, *Lymphopenic effects on mice of a component of ammonia caramel, 2-acetyl-4(5)-tetrahydroxybutylimidazole (THI).* Immunol Cell Biol, 1988. **66 (Pt 5-6)**: p. 395-402.
153. Houben, G.F., et al., *Effects of the colour additive caramel colour III on the immune system: a study with human volunteers.* Food Chem Toxicol, 1992. **30**(9): p. 749-57.
154. Schwab, S.R., et al., *Lymphocyte sequestration through S1P lyase inhibition and disruption of S1P gradients.* Science, 2005. **309**(5741): p. 1735-9.
155. Rivera, J., R.L. Proia, and A. Olivera, *The alliance of sphingosine-1-phosphate and its receptors in immunity.* Nat Rev Immunol, 2008. **8**(10): p. 753-63.
156. Bandhuvula, P., et al., *S1P lyase: a novel therapeutic target for ischemia-reperfusion injury of the heart.* Am J Physiol Heart Circ Physiol, 2011. **300**(5): p. H1753-61.
157. Kleinjan, A., et al., *Topical treatment targeting sphingosine-1-phosphate and sphingosine lyase abrogates experimental allergic rhinitis in a murine model.* Allergy, 2013. **68**(2): p. 204-12.
158. Nguyen-Tran, D.H., et al., *Molecular mechanism of sphingosine-1-phosphate action in Duchenne muscular dystrophy.* Dis Model Mech, 2014. **7**(1): p. 41-54.
159. Acharya, U., et al., *Modulating sphingolipid biosynthetic pathway rescues photoreceptor degeneration.* Science, 2003. **299**(5613): p. 1740-3.
160. German, O.L., et al., *Ceramide is a mediator of apoptosis in retina photoreceptors.* Invest Ophthalmol Vis Sci, 2006. **47**(4): p. 1658-68.
161. Sanvicens, N. and T.G. Cotter, *Ceramide is the key mediator of oxidative stress-induced apoptosis in retinal photoreceptor cells.* J Neurochem, 2006. **98**(5): p. 1432-44.
162. Ding, X.Q., et al., *Functional activity of photoreceptor cyclic nucleotide-gated channels is dependent on the integrity of cholesterol- and*

sphingolipid-enriched membrane domains. Biochemistry, 2008. **47**(12): p. 3677-87.
163. Miranda, G.E., et al., *Sphingosine-1-phosphate is a key regulator of proliferation and differentiation in retina photoreceptors.* Invest Ophthalmol Vis Sci, 2009. **50**(9): p. 4416-28.
164. Stone, J., et al., *Mechanisms of photoreceptor death and survival in mammalian retina.* Prog Retin Eye Res, 1999. **18**(6): p. 689-735.
165. Mustafi, D., A.H. Engel, and K. Palczewski, *Structure of cone photoreceptors.* Prog Retin Eye Res, 2009. **28**(4): p. 289-302.
166. Wright, A.F., *A searchlight through the fog.* Nat Genet, 1997. **17**(2): p. 132-4.
167. Piano, I., et al., *Cone survival and preservation of visual acuity in an animal model of retinal degeneration.* Eur J Neurosci, 2013. **37**(11): p. 1853-62.
168. Bradford, M.M., *A rapid and sensitive method for the quantitation of microgram quantities of protein utilizing the principle of protein-dye binding.* Anal Biochem, 1976. **72**: p. 248-54.
169. Laemmli, U.K., *Cleavage of structural proteins during the assembly of the head of bacteriophage T4.* Nature, 1970. **227**(5259): p. 680-5.
170. Munoz-Olaya, J.M., et al., *Synthesis and biological activity of a novel inhibitor of dihydroceramide desaturase.* ChemMedChem, 2008. **3**(6): p. 946-53.
171. Benzie, I.F. and J.J. Strain, *Ferric reducing/antioxidant power assay: direct measure of total antioxidant activity of biological fluids and modified version for simultaneous measurement of total antioxidant power and ascorbic acid concentration.* Methods Enzymol, 1999. **299**: p. 15-27.
172. Zarban, A., et al., *Antioxidant and radical scavenging activity of human colostrum, transitional and mature milk.* J Clin Biochem Nutr, 2009. **45**(2): p. 150-4.
173. Debien, E., et al., *S1PR5 is pivotal for the homeostasis of patrolling monocytes.* Eur J Immunol, 2013. **43**(6): p. 1667-75.
174. Arocho, A., et al., *Validation of the 2-DeltaDeltaCt calculation as an alternate method of data analysis for quantitative PCR of BCR-ABL P210 transcripts.* Diagn Mol Pathol, 2006. **15**(1): p. 56-61.
175. Yang, P., et al., *Oxidant-mediated Akt activation in human RPE cells.* Invest Ophthalmol Vis Sci, 2006. **47**(10): p. 4598-606.
176. Basu, A. and S. Haldar, *The relationship between Bcl2, Bax and p53: consequences for cell cycle progression and cell death.* Mol Hum Reprod, 1998. **4**(12): p. 1099-109.
177. Ma, Q., *Role of nrf2 in oxidative stress and toxicity.* Annu Rev Pharmacol Toxicol, 2013. **53**: p. 401-26.
178. Scarlatti, F., et al., *Resveratrol induces growth inhibition and apoptosis in metastatic breast cancer cells via de novo ceramide signaling.* FASEB J, 2003. **17**(15): p. 2339-41.
179. Roskoski, R., Jr., *ERK1/2 MAP kinases: structure, function, and regulation.* Pharmacol Res, 2012. **66**(2): p. 105-43.
180. Liu, C., et al., *Preconditioning with bright light evokes a protective response against light damage in the rat retina.* J Neurosci, 1998. **18**(4): p. 1337-44.

181. Dong, S.Q., et al., *Activation of the ERK 1/2 and STAT3 signaling pathways is required for 661W cell survival following oxidant injury.* Int J Ophthalmol, 2012. **5**(2): p. 138-42.
182. Toker, A. and S. Marmiroli, *Signaling specificity in the Akt pathway in biology and disease.* Adv Biol Regul, 2014.
183. Mo, M.S., et al., *PI3K/Akt and NF-kappaB activation following intravitreal administration of 17beta-estradiol: neuroprotection of the rat retina from light-induced apoptosis.* Neuroscience, 2013. **228**: p. 1-12.
184. Mackey, A.M., et al., *Redox survival signalling in retina-derived 661W cells.* Cell Death Differ, 2008. **15**(8): p. 1291-303.
185. Farrell, S.M., et al., *bFGF-mediated redox activation of the PI3K/Akt pathway in retinal photoreceptor cells.* Eur J Neurosci, 2011. **33**(4): p. 632-41.
186. Yung, H.W., D.S. Charnock-Jones, and G.J. Burton, *Regulation of AKT phosphorylation at Ser473 and Thr308 by endoplasmic reticulum stress modulates substrate specificity in a severity dependent manner.* PLoS One, 2011. **6**(3): p. e17894.
187. Takuwa, Y., et al., *Sphingosine-1-phosphate signaling in physiology and diseases.* Biofactors, 2012. **38**(5): p. 329-37.
188. Pettus, B.J., C.E. Chalfant, and Y.A. Hannun, *Ceramide in apoptosis: an overview and current perspectives.* Biochim Biophys Acta, 2002. **1585**(2-3): p. 114-25.
189. Cory, S., D.C. Huang, and J.M. Adams, *The Bcl-2 family: roles in cell survival and oncogenesis.* Oncogene, 2003. **22**(53): p. 8590-607.
190. Donovan, M., F. Doonan, and T.G. Cotter, *Decreased expression of pro-apoptotic Bcl-2 family members during retinal development and differential sensitivity to cell death.* Dev Biol, 2006. **291**(1): p. 154-69.
191. Rotstein, N.P., et al., *Protective effect of docosahexaenoic acid on oxidative stress-induced apoptosis of retina photoreceptors.* Invest Ophthalmol Vis Sci, 2003. **44**(5): p. 2252-9.
192. Benzie, I.F. and J.J. Strain, *The ferric reducing ability of plasma (FRAP) as a measure of "antioxidant power": the FRAP assay.* Anal Biochem, 1996. **239**(1): p. 70-6.
193. Tanito, M., M.P. Agbaga, and R.E. Anderson, *Upregulation of thioredoxin system via Nrf2-antioxidant responsive element pathway in adaptive-retinal neuroprotection in vivo and in vitro.* Free Radic Biol Med, 2007. **42**(12): p. 1838-50.
194. Prestera, T., et al., *Parallel induction of heme oxygenase-1 and chemoprotective phase 2 enzymes by electrophiles and antioxidants: regulation by upstream antioxidant-responsive elements (ARE).* Mol Med, 1995. **1**(7): p. 827-37.
195. German, O.L., et al., *Docosahexaenoic acid prevents apoptosis of retina photoreceptors by activating the ERK/MAPK pathway.* J Neurochem, 2006. **98**(5): p. 1507-20.
196. Chen, J., et al., *bcl-2 overexpression reduces apoptotic photoreceptor cell death in three different retinal degenerations.* Proc Natl Acad Sci U S A, 1996. **93**(14): p. 7042-7.

197. Betito, S. and O. Cuvillier, *Regulation by sphingosine 1-phosphate of Bax and Bad activities during apoptosis in a MEK-dependent manner.* Biochem Biophys Res Commun, 2006. **340**(4): p. 1273-7.
198. Yasuo, M., et al., *Fenretinide causes emphysema, which is prevented by sphingosine 1-phoshate.* PLoS One, 2013. **8**(1): p. e53927.
199. Li, Z., et al., *Astaxanthin protects ARPE-19 cells from oxidative stress via upregulation of Nrf2-regulated phase II enzymes through activation of PI3K/Akt.* Mol Vis, 2013. **19**: p. 1656-66.
200. Fan, J., et al., *Pharmacologic induction of heme oxygenase-1 plays a protective role in diabetic retinopathy in rats.* Invest Ophthalmol Vis Sci, 2012. **53**(10): p. 6541-56.
201. Min, K.S., et al., *Hydrogen peroxide induces heme oxygenase-1 and dentin sialophosphoprotein mRNA in human pulp cells.* J Endod, 2008. **34**(8): p. 983-9.
202. Strub, G.M., et al., *Extracellular and intracellular actions of sphingosine-1-phosphate.* Adv Exp Med Biol, 2010. **688**: p. 141-55.
203. van Echten-Deckert, G., et al., *cis-4-Methylsphingosine decreases sphingolipid biosynthesis by specifically interfering with serine palmitoyltransferase activity in primary cultured neurons.* J Biol Chem, 1997. **272**(25): p. 15825-33.

SCIENTIFIC PRODUCTS

Pubblications:

- In submission: Signorelli P.; Fabiani C.; Brizzolari A.; Paroni R.; Casas J., Fabriàs G.; Rossi D.; Ghidoni R.; Caretti A. “Natural grape extracts regulate colon cancer cells malignancy”, *Nutrition and Cancer.*
- The manuscript on thesis topic is in preparation.

Presentations on international events:

- The Association for research in vision and ophatlmology (ARVO) annual meeting, Seattle (WA, USA), May 5-9 2013.
  Poster presentation: “Inhibition of S1P degradation rescues 661W cells from oxidative stress”
- Sphingolipid Club Meeting 2013, Assisi (PG, Italy), June 27-30 2013.
  Oral presentation: “Inhibition of S1P degradation rescues 661W cells from oxidative stress”

RINGRAZIAMENTI

Un ringraziamento speciale è per il Professor Riccardo Ghidoni, per avermi seguito in questo percorso, per essere stato una tutore di dottorato ma soprattutto un punto di riferimento e una guida.

Inoltre vorrei ringraziare la Dott.ssa Paola Signorelli, per avermi aiutato costantemente a destreggiarmi nei meandri della biochimica degli sfingolipidi e non solo.

Un “grazie particolare”, va alla Dott.ssa Anna Caretti, per esserci sempre stata, per non essersi mai stancata di ascoltarmi anche quando gli interrogativi, scientific e non, si ripetevano incessamente.

Ovviamente, un “Grazie” è per tutto il laboratorio del 9° piano dell’Ospedale San Paolo di Milano, per avermi accolto e coccolato sin dall’inizio di questa avventura.: Nadia, Paola B., Rita P., Marco T., il Prof Michele Samaja e il Prof. Enzo Santaniello. In particolare, vorrei ringraziare tutte le *bimbe* e Andrea con cui ho condiviso gioie e dolori di questi anni milanesi.

Inoltre ringrazio la Prof.ssa Gemma Fabriàs, la Prof.ssa Josefina Casas e il loro laboratorio (iQAC, CSIC Barcellona, Spain) per il support tecnico ed il prezioso contributo. Infine vorrei ringraziare il Prof. Macchia e il suo gruppo dell’Università di Pisa per la proficua collaborazione di questi anni.